Theoretical and Applied Mechanics

University of Illinois at Urbana-Champaign

TAM

TAM Report No. 1042
UILU-ENG-2004-6003
ISSN 0073-5264

Asymptotic theory of ignition and failure of self-sustained detonations

by

Aslan R. Kasimov
D. Scott Stewart

February 2004

Asymptotic theory of ignition and failure of self-sustained detonations

Aslan R. Kasimov and D. Scott Stewart*
Department of Theoretical and Applied Mechanics,
University of Illinois at Urbana-Champaign, Urbana, IL 61801, USA

Based on a general theory of detonation waves with an embedded sonic locus that we have developed in Kasimov (2004) and Stewart & Kasimov (2004), we carry out asymptotic analysis of weakly-curved slowly-varying detonation waves and show that the theory predicts the phenomenon of detonation ignition and failure. The analysis is not restricted to near Chapman-Jouguet detonation speeds and is capable of predicting quasi-steady, normal detonation shock speed, curvature ($D-\kappa$) curves with multiple turning points. An evolution equation that retains the shock acceleration, $\dot{D}$, namely a $\dot{D}-D-\kappa$ relation is rationally derived and its solution for spherical (or cylindrical) detonation is shown to reproduce the ignition/failure phenomenon observed in both numerical simulations of blast wave initiation and in experiments. A simple physically transparent explanation of the ignition phenomenon is given in terms of the form of the evolution equation. A single-step chemical reaction described by one progress variable is employed, but the kinetics is sufficiently general and is not restricted to Arrhenius form, although most specific calculations in this work are performed for Arrhenius kinetics. As an example, we calculate critical energies of direct initiation for hydrogen-oxygen mixtures and find close agreement with available experimental data.

I. INTRODUCTION

During detonation in an explosive, the lead shock is maintained by the chemical energy release in the reaction zone. However the region that influences the shock and hence the reaction zone immediately behind the shock can be as large as the domain of the reacted products or as small as a reaction zone thickness. Self-sustained detonation waves are detonations whose dynamics are determined by a reaction zone of limited extent between the lead shock and a trailing sonic locus. The flow in the reaction zone between shock and sonic locus is isolated from the far-field flow, and acoustic disturbances on the downstream side of the sonic locus, which serves as a boundary, do not penetrate into the reaction zone. The sonic locus considered here is a characteristic surface and serves as an information boundary.

The simplest example of a self-sustained detonation is a plane, steady, Chapman-Jouguet (CJ) detonation (e.g. Fickett & Davis 1979) that when measured in the frame of the steady lead shock is sonic at the end of the reaction zone. Consider one-dimensional steady detonation. If one draws the forward (C_+) characteristics in a space-time plane traveling with the lead steady shock, the history line of the forward characteristic at the sonic point would be parallel to the history line of the lead shock, while forward characteristics between the shock and sonic point intersect the shock. The flow between the shock and sonic point is subsonic relative to the lead shock. The history lines of forward characteristics downstream of the sonic point are at most parallel to the shock or point away and do not intersect the shock or enter the reaction zone since the flow is supersonic. In contrast overdriven detonations require additional external support such as a piston to maintain the detonation structure at its nominal speed, and all forward characteristics intersect the lead shock.

Rational analyses of curved detonation have their origins in the study of the central problem of a steady detonation in a cylindrical stick of explosive (rate stick), identified by Eyring *et al.* (1949) in an attempt to explain the diameter effect, and a later analysis by Wood & Kirkwood (1954). In the analysis the radius of curvature of the lead shock was assumed to be large compared to the reaction zone. Generalized Chapman-Jouguet conditions were enforced at a point behind the shock to reflect the fact that the flow is sonic at some point in the reaction zone structure. Bdzil (1981) carried out the first consistent asymptotic analysis of the rate stick and used Lighthill's method of strained coordinate which invoked a regularity condition to derive a closure condition that was absent from the original Wood-Kirkwood analysis. Bdzil determined the axial detonation velocity in terms of the stick radius and the explosive properties and the confinement material properties.

Stewart & Bdzil (1988a) gave the first asymptotic derivation of the intrinsic relation between normal detonation shock speed, D_n and sum of the principal shock curvatures (or total curvature) κ and showed that that relationship

*Corresponding author; Electronic address: dss@uiuc.edu

depended only on the properties of the explosive. They also introduced the idea of slow time variation of the detonation dynamics, where time is measured on the scale of the particle passage time through the reaction zone. They used the method of matched asymptotic expansions to match the solution for the reaction zone structure in the near-shock layer to the solution in a transonic layer near the sonic point. Bdzil & Stewart (1988b, 1989) coined the word "Detonation Shock Dynamics" (DSD), to describe both the asymptotic theory associated with weak shock curvature and slow time evolution and the engineering application of the results to explosive systems. Klein & Stewart (1993) extended the work in Stewart & Bdzil (1988a) to consider reaction rate laws for Arrhenius kinetics with large activation energies. With a combination of distinguished asymptotic limits for large activation energy and numerics, Yao & Stewart (1995) and Stewart & Yao (1998) calculated the critical curvature and demonstrated that explosives with Arrhenius kinetics may have a quasi-steady detonation velocity, curvature relation in the shape of a Z with two, (an upper and lower) turning points. The normal detonation velocity-curvature curve has a high velocity branch that connects to the plane CJ value $D_n = D_{CJ}$ and a low velocity branch that connects asymptotically to a weakly reacting detonation with $D_n \sim c_0$, where c_0 is the ambient sound speed of the unreacted explosive.

An extension of the asymptotic theory to include higher order effects such as shock acceleration and time derivative of shock curvature was first considered by Yao & Stewart (1996), which gave results for pulsating and cellular gaseous detonation. Subsequently Stewart with Yao made an attempt at a revision of Yao & Stewart (1996), to develop a reduced theory, but due to confusion in regards to the nature of the sonic conditions and related difficulties with transonic-layer matching, the theory was left incomplete. Aslam, Bdzil & Hill (1998) calculated extensions to DSD theory that included both detonation acceleration and higher order transverse variations along the shock. Extension of DSD to steady detonation with two-step chemistry was carried out by Short & Bdzil (2003). All the works mentioned above have been based on the concept of "Master equation" where the definition of the sonic locus was identical to that in a steady wave, measured in the frame of the lead shock.

Generalization of the steady sonic-locus concept to unsteady detonations has been a problem that has been largely unaddressed. We have developed a general theory of detonation waves with an embedded sonic locus (Kasimov 2004; Stewart & Kasimov 2004) that applies to wide class of detonation waves in explosives with general equation of state and complex chemistry, and recently illustrated the behavior of the sonic locus by means of a numerical simulation in Kasimov & Stewart (2003). The sonic locus in general is unambiguously defined to be a characteristic surface that serves as a separatrix and an information boundary for the reaction zone initiated by the lead shock. Since it is characteristic, this boundary admits weak discontinuities in the gradients of flow variables in the normal direction to the surface. In the simplest one-dimensional case, the sonic locus is a separatrix of forward C_+ characteristic lines that remains at a finite non-zero distance from the shock at all times (Kasimov & Stewart 2003). We have shown that the sonic condition generalizes all previously known conditions that have been derived in asymptotic limits of weak curvature and slow time variation or have been used in linear stability studies of detonations in ideal gases as far-field boundary conditions (the so-called radiation conditions). The characteristic conditions require that the flow in the neighborhood of the sonic locus evolve smoothly. Of course in an asymptotic analysis, the conditions are approximated, starting from a general formulation.

The problem of detonation initiation, propagation and failure are the basic problems of detonation theory, which have implications for safety and performance of explosives and the engineering of explosive systems. Depending on the kind of sources used to initiate detonation, the explosive thermo-chemical properties, and geometrical constraints, one can ignite and propagate a self-sustained detonation. If certain critical conditions are not met the detonation fails. Direct initiation refers to detonation initiation of a main charge by a strong point-blast wave that is generated by an embedded smaller explosive charge, or energetic discharge from some other source such as an exploding bridge-wire. The ability to predict the critical conditions *a priori* is the ultimate goal of studies of detonation initiation.

Rational theoretical prediction of the critical conditions which would be based on the mixture constitutive properties only, has been a challenge in detonation theory, although variety of successful semi-empirical theories have been developed (e.g. Benedick et al 1986; Lee 1977; Lee 1984). In this work we derive a nonlinear evolution equation for a self-sustained detonation wave in the asymptotic limit of small curvature and slow-time variation, which are measured in the scales of steady reaction-zone length and time in the same sense of the previous DSD-theories. We assume that the detonation has an embedded sonic locus and employ the general characteristic conditions that we have developed in Kasimov (2004) and Stewart & Kasimov (2004). The equation retains the leading contributions from the shock curvature and shock acceleration. With a newly derived analytical formula not restricted to near Chapman-Jouguet speeds, we show that the quasi-steady form of the evolution equation exhibits a characteristic Z-shape curve in the space of the normal shock speed D_n and shock curvature κ that agrees closely with numerics. We show that the solution to the evolution equation that retains the shock acceleration, a $\dot{D}_n - D_n - \kappa$ relation, reproduces the ignition/failure phenomenon observed in both numerical simulations and in experiments on blast wave initiation in spherical (or cylindrical) geometries. We show that the critical energy of direct initiation provided by a strong point-

blast wave can be calculated and compares very well with available experimental data (Matsui & Lee 1979; Litchfield *et al.* 1962; Kaneshige *et al.* 1997).

Overview of the paper is as follows. We start with a general discussion of the governing equations in section 2, where we introduce the truncated Euler equations in the shock-attached frame, the Rankine-Hugoniot conditions, and scalings. Section 2.3 contains the leading-order planar quasi-steady solution of the Euler equations, while section 2.4 introduces a formulation of the governing equations in quasi-conserved variables with expansions of the state variables in small unsteady and curvature corrections in the main reaction layer. Sections 2.5 and 2.6 contain a discussion of the general sonic conditions in the unsteady detonation and a formulation in terms of the sonic frame. Section 3 contains a discussion of the sonic-frame expansions and coordinate matching with the shock-frame expansions. Section 3.3 derives the main results of the analysis, which are the compatibility condition and the speed relation which include the shock curvature and shock acceleration terms and yield an evolution equation for the detonation dynamics. Section 4.1 discusses main properties of the evolution equation, section 4.2 contains quasi-steady $D-\kappa$ solutions obtained analytically. The discussion of detonation ignition and failure is a subject of sections 4.3-4.5, where it is shown that the evolution equation that retains shock acceleration exhibits ignition and failure, and critical energies of direct initiation are calculated theoretically and compared against experiment. Section 5 discusses the large-activation energy form of the evolution equation. The section also contains a comparison of the theoretically computed $D-\kappa$ curve against the large-activation energy result as well as a numerically computed curve, which was obtained by solving the quasi-steady Euler equations numerically. Appendix A contains calculation of certain singular integrals in the evolution equation, while Appendix B explains the algorithm by which the numerical $D-\kappa$ curve is computed.

II. SIMPLIFIED GOVERNING EQUATIONS

We consider detonation waves with reaction zone structure that is slowly varying in time, measured on the particle passage time through the reaction zone, and that have lead shocks that have small curvature measured on reaction zone thickness. The two asymptotic assumptions (slow variation and weak curvature) are independent in general. It is not necessary to specify their relationship beforehand (that is choose a distinguished limit) in order to develop asymptotic approximations and the approximations can be treated separately. However the resulting order of the asymptotic approximations obtained depends on the size of terms that are neglected. Treating the approximations independently allows one to generate results that are quite general and have extended validity and include those obtained by using distinguished limits that relate the spatial and temporal scalings.

The equations we consider are the unsteady Euler equations written in the shock-attached frame, truncated to include terms proportional to the leading order shock curvature. The Rankine-Hugoniot conditions are applied at the lead shock. We also impose a boundary condition at the rear of the reaction zone on a limiting characteristic surface. The flow is exactly sonic for an observer traveling on the rear surface since it is characteristic. We call the rear limiting characteristic surface the "sonic" surface. The equations and boundary conditions form a closed system and allow for a solution that describes the motion of the detonation shock, the evolution of the material states in the reaction zone and the motion of the sonic surface. The reader can find a detailed derivation of the conditions at the sonic locus in Stewart & Kasimov (2004) and a derivation of a high-order evolution equation in Kasimov & Stewart (2004). Here we present a concise derivation of a simplified version of the evolution equation that retains the leading order curvature and shock acceleration corrections to the quasi-steady planar solution. The reduced equation and description still retains the basic physics involved in the ignition and failure phenomenon and leads to description of criticality, which is one of our main concerns in this paper.

A. Reduced Euler equations in the shock-attached frame

The Euler equations written in the shock-attached frame to $O(\kappa)$ are given by

$$\rho_t + (\rho U)_n + \kappa\rho\,(U+D) = 0, \tag{1}$$

$$U_t + UU_n + \dot{D} + vp_n = 0, \tag{2}$$

$$e_t + U e_n + p\,(v_t + U v_n) = 0, \tag{3}$$

$$\lambda_t + U\lambda_n = \omega\,. \tag{4}$$

The subscripts n and t denote partial differentiation with respect to spatial variable n which measures the distance from the shock into the reaction zone along a direction normal to the lead shock, and time t, respectively. The normal particle velocity in the shock-frame is $U = u - D$, u is the normal particle velocity in the lab frame, D is the normal shock velocity, $\dot{D}$ is the normal shock acceleration, p is pressure, $\rho = 1/v$ is density, v is the specific volume, e is the specific internal energy, λ is the reaction progress variable that goes form 0 at the shock to 1 at the end of reaction, ω is the reaction rate. We assume an ideal-gas equation of state and a one-step exothermic reaction that can be described by a single progress variable. Then $e = pv/(\gamma-1) - \lambda Q$, where γ is the polytropic exponent, Q is the heat of reaction. The sound speed squared for the ideal EOS is $c^2 = \gamma pv$. We do not need to specify the form of the reaction rate for much of the subsequent analysis, but later we will use the Arrhenius form to obtain formulas for quasi-steady response curves and describe the ignition and failure process.

Following Erpenbeck we use the ambient state to scale our variables, $\widetilde{p}_a$, $\widetilde{\rho}_a$, and $\sqrt{\widetilde{p}_a/\widetilde{\rho}_a}$ (tilde is used here to denote dimensional quantities). The length scale is the half-reaction length of a plane CJ detonation, $\tilde{l}_{1/2}$. The time scale is the ratio of the length scale to the velocity scale. Under this scaling the equations remain unchanged. The scaled values of upstream states (ρ, p, u, λ) are $(1,1,0,0)$ and the upstream sound speed squared for an ideal gas (with $\tilde{c}^2 = \gamma\tilde{p}\tilde{v}$) is $c^2 = \gamma$.

B. Rankine-Hugoniot algebra and shock boundary conditions

The Rankine-Hugoniot algebra connects the states in the reaction zone with conditions at the shock. Let $M = \rho U$ be the mass flux, $P = p + \rho U^2$ the momentum flux, and $H = e + pv + U^2/2 = c^2/(\gamma-1) + U^2/2 - \lambda Q$ be the specific enthalpy. Note that M, P and H are constant in the reaction zone for a steady state, plane detonation. Also the values of M, P and H in ambient unreacted explosive are the same as at the shock and are given by

$$M_0 = -D\,, \quad P_0 = 1 + D^2\,, \quad H_0 = \frac{\gamma}{\gamma-1} + \frac{D^2}{2}\,, \tag{5}$$

The pressure and velocity p and U can be expressed in terms of M and P as

$$p = P - M^2 v, \quad U = Mv, \tag{6}$$

Elimination of U and p in favor of v in the energy (Hugoniot) equation gives a quadratic for v (in the case of the ideal EOS)

$$v^2 - \frac{2\gamma}{\gamma+1}\frac{P}{M^2}v + \frac{2(\gamma-1}{(\gamma+1)}\frac{(H+\lambda Q)}{M^2} = 0\,. \tag{7}$$

One solves the quadratic to obtain

$$v = \frac{\gamma}{\gamma+1}\frac{P}{M^2}\,(1-\delta)\,, \tag{8}$$

where

$$\delta^2 = 1 - \frac{hM^2}{P^2}\,(H+\lambda Q)\,, \quad \text{and} \quad h = \frac{2(\gamma^2-1)}{\gamma^2}\,, \tag{9}$$

which holds throughout the reaction zone structure.

If we introduce the normal Mach number (squared) in the shock-attached frame

$$\mathsf{M}^2 = \frac{U^2}{c^2}\,, \tag{10}$$

then some simple algebra shows that δ^2 can also be re-written compactly as

$$\delta^2 = 1 - h\frac{M^2}{P^2}\,(H+\lambda Q) = \left(\frac{1-\mathsf{M}^2}{1+\gamma\mathsf{M}^2}\right)^2. \tag{11}$$

This illustrates that the argument of the square root that defines δ is positive. Thus, the argument of the square root is a perfect square and can vanish only at points where the Mach number M measured in the shock frame is unity.

The CJ detonation velocity D_{CJ} corresponds to the case of a plane, steady detonation with complete reaction at the sonic point, where $\mathsf{M}^2 = 1$. In this case one sets $\delta = 0$ at $\lambda = 1$ with $M = -D$, $P = 1+D^2$ and $H = \gamma/(\gamma-1)+D^2/2$ and derives a quadratic for D^2 with solution

$$D_{CJ} = \sqrt{\gamma+q}+\sqrt{q}, \quad \text{where} \quad q = \left(\gamma^2-1\right)Q/2. \tag{12}$$

C. The quasi-steady planar solution

The quasi-steady planar solution corresponds to the leading order solution that ignores curvature and shock acceleration terms (i.e $\dot{D} = 0$, $\kappa = 0$). The solution for the leading order state variables is given by the solution to the Rankine-Hugoniot conditions discussed above. Hence the leading order quasi-steady approximation, denoted with a 0-subscript is given by

$$\rho_0 = \frac{\gamma+1}{\gamma}\frac{D^2}{1+D^2}\frac{1}{1-\delta_0}, \tag{13}$$

$$p_0 = \frac{1+D^2}{\gamma+1}\,(1+\gamma\delta_0)\,, \tag{14}$$

$$U_0 = -\frac{\gamma}{\gamma+1}\frac{1+D^2}{D}\,(1-\delta_0)\,, \tag{15}$$

where after a little bit of algebra δ_0^2 can be expressed as

$$\delta_0^2 = 1 - h\frac{M_0^2}{P_0^2}\,(H_0+\lambda_0 Q) = b^2\,(1+F-\lambda_0) \tag{16}$$

where

$$b = \frac{D(D_{CJ}^2-\gamma)}{\gamma D_{CJ}(1+D^2)}, \quad F = \left(D^2-D_{CJ}^2\right)\frac{D^2D_{CJ}^2-\gamma^2}{D^2\left(D_{CJ}^2-\gamma\right)^2}, \tag{17}$$

which simplify further calculations. The leading order spatial distribution of reactants λ_0 is given by

$$n = \int_0^{\lambda_0}\frac{U_0\,d\bar{\lambda}_0}{\omega_0}\,. \tag{18}$$

It is easy to see that if $D \geq D_{CJ}$, that if the detonation is overdriven, then $F \geq 0$. For the under-driven detonation, that is if $D < D_{CJ}$, hence $F < 0$, the quasi-steady planar sonic locus is located at $\delta_0 = 0$ at a point of an incomplete burning, $\lambda_{0*} = 1+F$. Function F has a property that its minimum value is -1 irrespective of D_{CJ} and γ and so λ_{0*} is well defined for all D. Also, F is negative for $\sqrt{\gamma} < D < D_{CJ}$ and positive for $D > D_{CJ}$. This quasi-steady solution is used below for derivation of an evolution equation that includes shock acceleration and curvature, as a basic-state solution, that is as a first approximation in an asymptotic expansion.

D. Formulation in conserved variables in the shock-attached frame

The variables M, P and H have special property that they are constant for a steady, plane detonation. For this reason, we call them "conserved variables", although in general unsteady detonation they are not conserved. In a multidimensional, unsteady analysis that deviates from the plane solutions, one looks for corrections to these constants. The reduced governing equations re-written in terms of M, P, H and λ, are

$$M_n = -\rho_t - \kappa\rho\,(U+D)\,, \tag{19}$$

$$P_n = -M_t - \rho\dot{D} - \kappa\rho U\,(U+D)\,, \tag{20}$$

$$H_n = -\frac{H_t}{U} - \dot{D} + \frac{v}{U}p_t, \tag{21}$$

$$\lambda_t + U\lambda_n = \omega. \tag{22}$$

Approximations that assume weak shock curvature and slow time variation seek to find corrections to the constant values of M, P and H as well as to a steady-state reactant distribution. Specifically the left-hand sides of (19), (20) and (21) when integrated across the reaction zone structure generate a small correction to the values of M, P and H evaluated at the shock. The spatially integrated form of the governing equations are a system of integro-differential equations for M, P and H and λ. Specifically, if we integrate from the shock at $n = 0$ to a point in the reaction zone and apply the shock condition, we obtain

$$M = M_0 + M_1\,, \quad P = P_0 + P_1\,, \quad H = H_0 + H_1\,, \tag{23}$$

where

$$M_1 = -\int_0^n \rho_t dn - \kappa\int_0^n \rho\,(U+D)\,dn, \tag{24}$$

$$P_1 = -\int_0^n \left(M_t + \rho\dot{D}\right) dn - \kappa\int_0^n \rho U\,(U+D)\,dn, \tag{25}$$

$$H_1 = \int_0^n \left(-\frac{H_t}{U} - \dot{D} + \frac{p_t}{M}\right) dn. \tag{26}$$

In this form the corrections are exact, but with the assumptions of weak curvature and slow variation, they can be regarded to be asymptotically small. In a similar manner, one can integrate the rate equation. The approach is to estimate integrals in M_1, P_1, H_1 and then invert the Rankine-Hugoniot algebra to compute the primitive states. Importantly the shock boundary conditions are applied exactly with precision to all orders and expansions generated by approximation have validity in the main reaction layer (MRL) that has the shock as the boundary.

Likewise, if the curvature and unsteady corrections are small we can generate expansions in the MRL by using the expressions for M, P and H, inserting them into formulas for δ, (9), v, (8), then for U and p (6). In particular, since δ vanishes to leading order as we approach the end of the reaction zone for a CJ detonation we postpone expanding it, since it changes order. Later we will see that this is required to generate a uniform asymptotic expansion. But by expanding M and P and retaining δ as an unexpanded (treated as an $O(1)$) quantity to be expanded later, we generate an MRL-expansion for v

$$v^{MRL} = \frac{\gamma}{\gamma+1}\frac{P}{M^2}\,(1-\delta) = \frac{\gamma}{\gamma+1}\frac{P_0}{M_0^2}\left(1 + \frac{P_1}{P_0} - \frac{2M_1}{M_0} - \delta\right) + \ldots, \tag{27}$$

with corresponding expansions for U^{MRL} and p^{MRL}. In the simplest case, when one uses the definitions of M_0, P_0 and H_0 (5), drops the time dependent contributions to M_1, P_1 and H_1, only retaining the curvature corrections and approximates the integrals with the plane, CJ, steady state, then the MRL expansions found in Stewart & Bdzil (1988a) and Klein & Stewart (1993) are obtained with this simple expansion of the algebraic form. Thus the effects of unsteady and curvature terms can be included as corrections to the constant steady solution.

The apparent simplicity of the approach is deceiving as the right-hand sides of the governing equations will contain expressions involving the square root defined in equation (9). As it turns out (for more details, see Kasimov 2004; Stewart & Kasimov 2004), most of the difficulties associated with approximating the structure of detonations with an embedded sonic locus have to do with this square root. An obvious difficulty is seen immediately by observing that for the steady detonation the argument of the square root vanishes at the sonic point. Since the governing equations contain time derivatives of v and hence of the square root, then terms having the inverse of the square root will appear, which are potentially singular at points where the square root vanishes.

The function δ itself is a perfectly regular function and has no singularities anywhere in the flow. But as soon as we expand it, we immediately obtain terms that are inversely proportional to powers of the square-root obtained from equation (9) which become singular as the argument of the square root vanishes. A simple example of such a function is $\sqrt{x+\varepsilon}$, which when expanded in small ε becomes $\sqrt{x}(1+\varepsilon/2x+o(\varepsilon))$. Clearly, the singularity at $x=0$ is a result of the expansion of a function which is non-uniform, that is the function behaves like $\sqrt{x}+O(\varepsilon)$ at $x \gg \varepsilon$, while for $x \ll \varepsilon$ the leading-order term of the function is $\sqrt{\varepsilon}$. The multiple-scale character of this simple function mimics the behaviour of a detonation wave with a sonic locus as a multiple-scale phenomenon. Problems associated with this apparent singularity in analytical treatments have been a central challenge in the theory developed to date.

E. Characteristic conditions at the sonic locus

In a recent work we demonstrated via high resolution computation, the nature of self-sustained detonations with an embedded sonic locus behind the shock, Kasimov & Stewart (2003). In Stewart & Kasimov (2004) we worked out the general three-dimensional formulation for this surface as a rear boundary condition. The sonic locus is coincident with a forward propagating characteristic surface that remains at a finite distance behind the lead shock throughout the evolution. Forward propagation is defined in terms of the component of velocity normal to the surface that points toward the lead shock, and described in a one-dimensional context is usually associated with a C_+ forward characteristic. Such a "sonic locus" is a separatrix that separates the family of forward characteristic surfaces into ones that intersect the shock in a finite time, (i.e. are in a region that is subsonic) and characteristic surfaces that flow away from the shock and never intersect it. There are two fundamental properties of the sonic locus that is coincident with a characteristic surface: the normal Mach number defined in terms of the normal particle speed for an observer in the surface is unity; there is a differential constraint on the evolution of states in the surface that in a one-dimensional isentropic context derives the Riemann invariant. The first constraint defines the normal speed of the sonic locus and hence we refer to it as the "speed relation". The second constraint is known in the theory of characteristics as the "compatibility condition" and we use these names throughout. A one-dimensional sketch of the sonic locus discussed here is shown in figure 1.

For purposes of illustrating these two conditions we imagine that we choose a point on the lead shock and draw a normal along it, and then take the x-axis in the laboratory frame coincident with that normal. Then we can write the relation between the lab-frame position, x, shock position $x_s(t)$ and distance measured from the shock n as

$$x = x_s(t) + n\,. \tag{28}$$

Next simply write equations (1)-(4) in characteristic form, then the equations on the forward C_+ characteristic obey the differential relation

$$\dot{p}_* + \rho_* c_* \dot{u}_* + \kappa \rho_* c_*^2 u_* = (\gamma - 1) Q \rho_* \omega_*, \tag{29}$$

on

$$\frac{dx_*}{dt} = u_* + c_*\,. \tag{30}$$

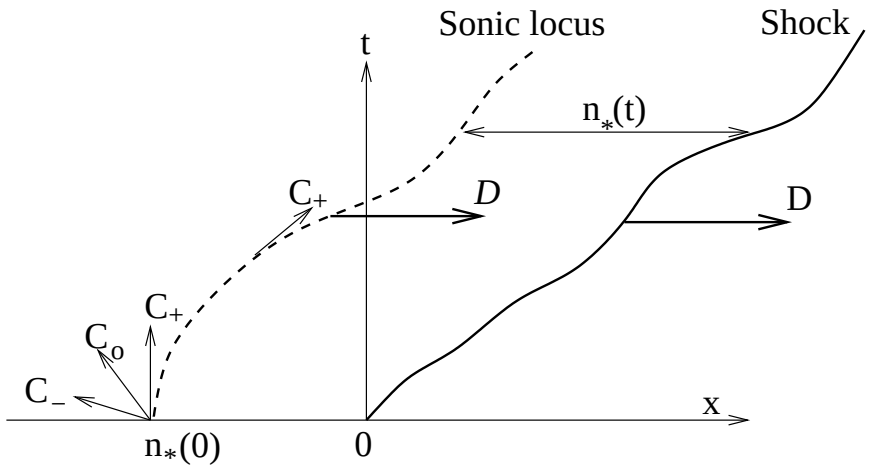

Figure 1: $x-t$ diagram of the shock locus and the sonic locus in self-sustained one-dimensional planar detonation.

where we have evaluated these relations on the sonic locus denoted by a * subscript. If we differentiate the coordinate transformation on the sonic locus, $x_* = x_s(t) + n_*(t)$ with respect to time to obtain, $dx_*/dt = D + \dot{n}_*$, we can represent the expression of the characteristic speed (30) in the lab-frame to that expressed in the shock-attached frame as

$$\dot{n}_* = c_* + U_* \,, \tag{31}$$

that is an explicit formula for the normal speed of the sonic locus relative to the shock ($U_* = u_* - D$). The characteristic conditions can of course be expressed in any frame, as is convenient. We refer to (29) as the *compatibility condition* and (31) as the *speed relation*. These conditions applied on the sonic locus are boundary conditions that determine both the motion of the sonic surface and the states on it. Since the sonic locus is a separatrix of characteristics, then the flow between the shock and sonic locus is entirely determined by the data in the domain of influence between the shock and sonic locus.

Since the normal Mach number in the shock-attached frame is $\mathsf{M} = -U/c$, then an important observation is that on the sonic surface, the shock frame Mach number can be expressed as

$$\mathsf{M}_* = 1 - \frac{\dot{n}_*}{c_*}, \tag{32}$$

that is, the sonic Mach number defined in terms of the shock-frame velocity can vary around unity depending on whether the sonic locus is moving toward ($\dot{n}_* > 0$) or away from the shock ($\dot{n}_* < 0$). This is where a departure from previous theories that define the trailing sonic locus as a point where the shock-frame Mach number is one, i.e. $\mathsf{M}_* = 1$ takes place. We can see that slow time variation associated with the motion of the sonic locus enters the analysis through in particular the magnitude of the relative velocity of the shock and sonic surface, $\dot{n}_*$.

By inserting (32) into (8) one obtains an important *exact* expression at the sonic point,

$$\delta_* = \frac{1}{1+\gamma\mathsf{M}_*^2} \frac{\dot{n}_*}{c_*} \left(2 - \frac{\dot{n}_*}{c_*}\right), \tag{33}$$

that later will be used to uniformly approximate the magnitude of δ_* in the transonic-layer matching.

F. Sonic-frame formulation

Next we consider a description of the detonation structure as viewed by an observer attached to the frame of the sonic locus. Let N be a new spatial variable that measures distance along the shock normal from the sonic surface,

$N = n - n_*(t)$. Let $\mathcal{D}$ be the normal speed of the sonic locus as measured in the lab-frame and $\mathcal{U} = u - \mathcal{D}$ be the particle velocity in the sonic-locus frame. We also introduce new conserved variables

$$\mathcal{M} = \rho\,\mathcal{U},\ \mathcal{P} = p + \rho\,\mathcal{U}^2,\ \mathcal{H} = \frac{c^2}{\gamma - 1} + \frac{\mathcal{U}^2}{2} - \lambda Q. \tag{34}$$

Then the governing equations in these variables are also similar to their counterparts in the shock frame, and it is easy to verify that the governing equations are

$$\mathcal{M}_N = -\rho_t - \kappa\rho\,(\mathcal{U} + \mathcal{D}), \tag{35}$$

$$\mathcal{P}_N = -\mathcal{M}_t - \rho\dot{\mathcal{D}} - \kappa\rho\,\mathcal{U}(\mathcal{U} + \mathcal{D}), \tag{36}$$

$$\mathcal{H}_N = -\frac{\mathcal{H}_t}{\mathcal{U}} - \dot{\mathcal{D}} + \frac{v}{\mathcal{U}} p_t, \tag{37}$$

$$\lambda_N = \frac{1}{\mathcal{U}}(\omega - \lambda_t). \tag{38}$$

The primitive variables can be expressed in terms of these new ones as

$$v = \frac{\gamma}{\gamma+1}\frac{\mathcal{P}}{\mathcal{M}^2}\,(1 - \Delta), \quad p = \frac{\mathcal{P}}{\gamma+1}\,(1 + \gamma\Delta), \quad \mathcal{U} = \mathcal{M} v, \tag{39}$$

where now

$$\Delta = \sqrt{1 - \frac{h\mathcal{M}^2}{\mathcal{P}^2}\,(\mathcal{H} + \lambda Q)}. \tag{40}$$

Also, similar to that in the shock frame, we again have the equation

$$\Delta^2 = 1 - \frac{h\mathcal{M}^2}{\mathcal{P}^2}\,(\mathcal{H} + \lambda Q) = \left(\frac{1 - \mathtt{M}^2}{1 + \gamma\mathtt{M}^2}\right)^2, \tag{41}$$

where $\mathtt{M} = -\mathcal{U}/c$ is now the normal Mach number *relative to the sonic locus*, with the important difference that this time $\mathtt{M}_* = 1$ is imposed as an *exact* condition on that surface, which as one can see from (41) also corresponds to

$$\Delta_* = 0. \tag{42}$$

Equations (35)-(38) can also be integrated from $N = 0$ (on the sonic locus) to an arbitrary point N in the structure to obtain integro-differential equations. An important difference from the shock-frame formulation is that we impose the boundary conditions $\mathcal{M} = \mathcal{M}_*$, $\mathcal{P} = \mathcal{P}_*$ and $\mathcal{H} = \mathcal{H}_*$ to all orders (that is exactly) at the sonic locus instead of at the shock. And like the approximations in the main reaction layer, that are formulated with the shock as the boundary, we will generate approximations in the transonic layer (TSL).

III. SLOW-TIME AND WEAK-CURVATURE ANALYSIS

To obtain the evolution equations for the shock and sonic locus, at some asymptotic order we approximate the flow states variables at the sonic locus and substitute them into the compatibility condition (29) and the speed relation (31). In order to calculate the states at the sonic locus we use a method of successive approximation to generate asymptotic expansions, first employed in Yao & Stewart (1996) and recently by us in Kasimov & Stewart (2004) .

A. Transonic layer expansion in the sonic frame

Near the sonic locus we develop a coordinate expansion of the solution in the sonic frame, expressed in the variable $N = n - n_*$ in the limit $N \to 0$. This solution must match with an expansion in the main reaction layer (MRL) as $n \to n_*$. Matching provides the connection between the TSL and MRL layers, and allows us to derive the asymptotic formulas for structure and the dynamics of the detonation structure.

We write the governing system in the sonic frame as follows

$$\mathcal{M} = \mathcal{M}_* - \int_0^N \rho_t dN - \kappa \int_0^N \rho\,(\mathcal{U} + \mathcal{D})\, dN, \tag{43}$$

$$\mathcal{P} = \mathcal{P}_* - \int_0^N \left(\mathcal{M}_t + \rho\dot{\mathcal{D}}\right) dN - \kappa \int_0^N \rho\,\mathcal{U}\,(\mathcal{U} + \mathcal{D})\, dN, \tag{44}$$

$$\mathcal{H} = \mathcal{H}_* + \int_0^N \left(-\frac{\mathcal{H}_t}{\mathcal{U}} - \dot{\mathcal{D}} + \frac{v}{\mathcal{U}} p_t\right) dN, \tag{45}$$

$$\lambda_N = \frac{1}{\mathcal{U}}(\omega - \lambda_t). \tag{46}$$

In this form the system is exact. The leading order terms $\mathcal{M}_*$, $\mathcal{P}_*$, and $\mathcal{H}_*$ are *exact* values evaluated at the sonic locus. If we denote

$$\mathcal{M}_1 = -\int_0^N \rho_t dN - \kappa \int_0^N \rho\,(\mathcal{U} + \mathcal{D})\, dN,$$

$$\mathcal{P}_1 = -\int_0^N \left(\mathcal{M}_t + \rho\dot{\mathcal{D}}\right) dN - \kappa \int_0^N \rho\,\mathcal{U}\,(\mathcal{U} + \mathcal{D})\, dN,$$

and

$$\mathcal{H}_1 = \int_0^N \left(-\mathcal{H}_t/\mathcal{U} - \dot{\mathcal{D}} + v p_t/\mathcal{U}\right) dN,$$

then we write

$$\mathcal{M} = \mathcal{M}_* + \mathcal{M}_1, \quad \mathcal{P} = \mathcal{P}_* + \mathcal{P}_1, \quad \mathcal{H} = \mathcal{H}_* + \mathcal{H}_1. \tag{47}$$

The terms $\mathcal{M}_1, \mathcal{P}_1$ and $\mathcal{H}_1$ that contain time derivatives and terms proportional to the shock curvature can be considered as corrections to the leading order terms.

The corrections $\mathcal{M}_1, \mathcal{P}_1$ and $\mathcal{H}_1$ in the TSL can be expanded uniformly to obtain

$$\mathcal{M}_1 = -\int_0^N \rho_t dN = -\rho_{*t} N - \kappa\rho_*\,(\mathcal{U}_* + \mathcal{D})\, N + O(N^2), \tag{48}$$

$$\mathcal{P}_1 = -\left(\mathcal{M}_{*t} + \rho_*\dot{\mathcal{D}}\right) N - \kappa\rho_*\,\mathcal{U}_*\,(\mathcal{U}_* + \mathcal{D})\, N + O(N^2), \tag{49}$$

$$\mathcal{H}_1 = \left(-\frac{\mathcal{H}_{*t}}{\mathcal{U}_*} - \dot{\mathcal{D}} + \frac{1}{M_*} p_{*t}\right) N + O(N^2), \tag{50}$$

Also let $\lambda = \lambda_* + \lambda_1$ and by integrating the rate equation in the sonic frame for small N, we obtain

$$\lambda = \lambda_* + \int_0^N \frac{1}{\mathcal{U}} (\omega - \lambda_t)\, dN = \lambda_* + \frac{1}{\mathcal{U}_*} (\omega_* - \lambda_{*t})\, N + O(N^2), \tag{51}$$

with λ_1 identified as

$$\lambda_1 = \frac{1}{\mathcal{U}_*} (\omega_* - \lambda_{*t})\, N. \tag{52}$$

Notice that in reducing the above expressions we replaced $(\rho_t)_*$ with $(\rho_*)_t = d\rho_*/dt$ and similarly with other time derivatives evaluated at the sonic locus. This is justified since at the sonic locus $d/dt = \partial/\partial t + (c_* + \mathcal{U}_*)\,\partial/\partial N = \partial/\partial t$ which holds because $c_* + \mathcal{U}_* = 0$.

We can now evaluate the spatial expansion of v. First, let us find the expansion of Δ,

$$\Delta^2 = 1 - \frac{2(\gamma^2-1)}{\gamma^2} \frac{(\mathcal{M}_* + \mathcal{M}_1)^2}{(\mathcal{P}_* + \mathcal{P}_1)^2} (\mathcal{H}_* + \lambda_* Q + \mathcal{H}_1 + \lambda_1 Q) + o(\mathcal{M}_1, \mathcal{P}_1, \mathcal{H}_1, \lambda_1). \tag{53}$$

Using $\Delta_* = 0$, we obtain

$$\Delta^2 = -\frac{\mathcal{H}_1 + \lambda_1 Q}{\mathcal{H}_* + \lambda_* Q} - 2\left(\frac{\mathcal{M}_1}{\mathcal{M}_*} - \frac{\mathcal{P}_1}{\mathcal{P}_*}\right) + h.o.t. \tag{54}$$

We now take advantage of the following exact expressions

$$v_* = \frac{\gamma}{\gamma+1}\frac{\mathcal{P}_*}{\mathcal{M}_*^2}, \quad p_* = \frac{\mathcal{P}_*}{\gamma+1}, \quad \mathcal{U}_* = \frac{\gamma}{\gamma+1}\frac{\mathcal{P}_*}{\mathcal{M}_*} = -c_*, \tag{55}$$

and

$$\mathcal{H}_* + \lambda_* Q = \frac{\gamma+1}{2(\gamma-1)}\mathcal{U}_*^2, \quad \rho_* = \frac{\gamma}{\gamma+1}\frac{\mathcal{P}_*}{\mathcal{U}_*^2}, \quad \mathcal{M}_* = \frac{\gamma}{\gamma+1}\frac{\mathcal{P}_*}{\mathcal{U}_*}, \tag{56}$$

$$\dot{\rho}_* = \frac{\gamma}{\gamma+1}\left(\frac{\dot{\mathcal{P}}_*}{\mathcal{U}_*^2} - \frac{2\mathcal{P}_*\dot{\mathcal{U}}_*}{\mathcal{U}_*^3}\right), \quad \dot{\mathcal{M}}_* = \frac{\gamma}{\gamma+1}\left(\frac{\dot{\mathcal{P}}_*}{\mathcal{U}_*} - \frac{\mathcal{P}_*\dot{\mathcal{U}}_*}{\mathcal{U}_*^2}\right). \tag{57}$$

Inserting these expressions into (54), after some algebra we obtain

$$\Delta^2 = -\frac{2}{\gamma+1}\frac{1}{c_*^2}\left[\dot{u}_* + \frac{\dot{p}_*}{\rho_* c_*}\right] N - \frac{2\kappa}{\gamma+1}\frac{u_*}{c_*} N + Q\frac{\dot{\lambda}_*/\mathcal{U}_* \cdot N + \lambda_1}{\mathcal{H}_* + \lambda_* Q} + O(N^2). \tag{58}$$

Also using (52) it follows that

$$Q\frac{\dot{\lambda}_*/\mathcal{U}_* \cdot N + \lambda_1}{\mathcal{H}_* + \lambda_* Q} = -\frac{2(\gamma-1)}{\gamma+1}\frac{Q}{c_*^2}\frac{\omega_*}{c_*} N + O(N^2). \tag{59}$$

Combining all terms in (58) together results in the following spatial expansion for Δ^2,

$$\Delta^2 = -\frac{2}{\gamma+1}\frac{1}{\rho_* c_*^3}\left[\dot{p}_* + \rho_* c_* \dot{u}_* - (\gamma-1)\rho_* Q\omega_* + \kappa\rho_* c_*^2 u_*\right] N + O(N^2). \tag{60}$$

Remarkably, we find that *the leading order spatial expansion of* Δ^2 *proportional to* $O(N)$ *is proportional to the compatibility condition*, i.e. the expression of the forward characteristic relation expressed on the sonic locus. Since the sonic locus is characteristic, the compatibility condition is identically satisfied, and so the terms in square brackets in (60) vanish. Hence, the sonic frame expansion of v is given by

$$v^{TSL} = v_* \left[1 + \frac{\mathcal{P}_1}{\mathcal{P}_*} - \frac{2\mathcal{M}_1}{\mathcal{M}_*} - \Delta \right] + ... = v_* + O(N). \tag{61}$$

The fact that the expansion of Δ^2 starts with $O(N^2)$ terms and that $O(N)$ terms are absent can be derived in a different way. Since the spatial derivative of v (and hence p and U) contains a term proportional to

$$\frac{\partial \Delta}{\partial N} = \frac{1}{2\Delta} \frac{\partial \Delta^2}{\partial N} \tag{62}$$

and at the sonic point $\Delta_* = 0$, it must also be true that $\left(\partial\Delta^2/\partial N\right)_* = 0$ if the derivatives of the state variables are to remain finite. Direct calculation of $\left(\partial\Delta^2/\partial N\right)_*$ shows that indeed it is proportional to the compatibility condition and hence vanishes at the sonic locus. Thus we come to an important conclusion that *the compatibility condition (which is fundamental) is also a regularity condition for the derivatives of the state variables at the sonic point*. In other words, on the sonic surface, the spatial and temporal derivatives of the state variables must be finite.

B. Spatial matching of the Main Reaction Layer and Transonic Layer

To demonstrate the matching of the MRL and TSL expansions we expand v^{MRL} given by (27) in the limit as $n \to n_*$ and compare it to v^{TSL} in (61) as $N \to 0$. Specifically we write $n = n_* + \Delta n$ and evaluate the integrals in equations (24)-(26) at $n = n_* + \Delta n$, where $\Delta n \equiv N \to 0$ to obtain the expansions

$$M = M_0 + M_{1*} + O(\Delta n), \quad P = P_0 + P_{1*} + O(\Delta n), \quad H = H_0 + H_{1*} + O(\Delta n). \tag{63}$$

We substitute these into equation (27) and obtain

$$v^{MRL} = \frac{\gamma}{\gamma+1} \frac{1+D^2}{D^2} \left(1 + \frac{P_{1*}}{P_0} - \frac{2M_{1*}}{M_0} - \delta_* \right) + O(\Delta n). \tag{64}$$

Notice M_{1*}, P_{1*}, H_{1*} and δ_* are functions of time. We do not expand δ but rather use its *exact* value at the sonic point, which leaves the truncated terms at $O(\Delta n)$. Note again that δ is uniformly regular as $\Delta n \to 0$ while its expansion is not. Spatial matching of the TSL and MRL to leading order obtains the sonic state specific volume

$$v_* = \frac{\gamma}{\gamma+1} \frac{1+D^2}{D^2} \left(1 + \frac{P_{1*}}{P_0} - \frac{2M_{1*}}{M_0} - \delta_* \right). \tag{65}$$

The pressure at the sonic locus, p_* is given simply by

$$p_* = \frac{1+D^2}{\gamma+1} \left(1 + \frac{P_{1*}}{P_0} + \gamma\delta_* \right). \tag{66}$$

Using $\mathcal{U}_* = -c_* = -\sqrt{\gamma p_* v_*}$, we can find the sonic-frame particle velocity,

$$\mathcal{U}_* = -\frac{\gamma}{\gamma+1} \frac{1+D^2}{D} \left(1 + \frac{P_{1*}}{P_0} - \frac{M_{1*}}{M_0} + \frac{\gamma-1}{2}\delta_* \right). \tag{67}$$

Next the sonic states listed above are computed to include corrections to $O\left(\dot{D}, \kappa, \dot{n}_*\right)$. Then the compatibility condition and speed relation are imposed at the sonic locus. To complete the analysis we must consider contributions to the integrals that require consideration of the rate equation. We proceed to these calculations next and derive equations for the main unknowns of the problem, D, λ_* and n_*.

C. Calculation of the compatibility condition and the speed relation

Here we evaluate the integrals M_{1*}, P_{1*}, and H_{1*} to the leading leading order corrections in $\partial/\partial t$ and κ, in order to compute the sonic state variables. Then we substitute the result into the sonic conditions to obtain a reduced evolution system for the shock dynamics.

First consider the compatibility condition. To obtain terms up to $O(\dot{D},\kappa)$ we only need the leading-order quasi-steady, planar solution since the compatibility condition is a differential relation. The leading order sonic-state is given by

$$p_{0*} = \frac{1+D^2}{\gamma+1}, \quad v_{0*} = \frac{\gamma}{\gamma+1}\frac{1+D^2}{D^2}, \quad c_{0*} = -U_{0*} = \frac{\gamma}{\gamma+1}\frac{1+D^2}{D}, \tag{68}$$

so that

$$\rho_{0*}c_{0*} = D, \quad u_{0*} = -c_{0*} + D + \dot{n}_* = \frac{D^2-\gamma}{(\gamma+1)D}. \tag{69}$$

Then we find that to $O(\dot{D},\kappa)$,

$$\dot{p}_* = \frac{2D\dot{D}}{\gamma+1}, \quad \dot{u}_* = \frac{D^2+\gamma}{(\gamma+1)D^2}\dot{D}, \quad \kappa\rho_* c_*^2 u_* = \kappa\frac{\gamma}{(\gamma+1)^2}\frac{(1+D^2)(D^2-\gamma)}{D}. \tag{70}$$

Notice that $\dot{n}_*$ is absent in (70) because it comes in only through the derivative of δ_*, which is $o(\dot{n}_*)$ and so is of higher order than we retain here. Substitution of (70) into the compatibility condition (29) results in an equation relating $\dot{D}$, D, κ, and λ_*,

$$\dot{D} = a_1\omega_* - a_2\kappa, \tag{71}$$

where

$$a_1 = \frac{\gamma+1}{\gamma}\frac{(\gamma^2-1)QD^3}{(1+D^2)(\gamma+3D^2)}, \quad a_2 = \frac{\gamma}{\gamma+1}\frac{(1+D^2)(D^2-\gamma)}{\gamma+3D^2}. \tag{72}$$

One immediate observation from equation (71) is that if $\dot{D}$ is neglected (corresponding to quasi-steady *curved detonation*), the equation has no solution with negative curvature for one-step exothermic reaction (that is for $\omega_* \geq 0$), which implies that for this type of chemistry, no quasi-steady converging detonation wave with a sonic locus can exist. Clearly, if more complex kinetics is considered such that ω_* can be negative, then quasi-steady converging ($\kappa < 0$) detonation is possible.

Next we evaluate the speed relation. Since the speed relation is algebraic in state variables, we need to compute the sonic states including the integral corrections, which give $O\left(\dot{D},\kappa\right)$ contributions. The original speed relation is $\dot{n}_* = c_* + U_*$, or which is the same, $\mathrm{M}_* = 1 - \dot{n}_*/c_*$. We will use an equivalent relation that is written in terms of the conserved variables, for which we have simple asymptotic expansions. Such a relation is provided by equation (11) that relates all conserved variables to the Mach number M. Also recall that we have an exact expression for δ_* in terms of $\dot{n}_*$ provided by equation (33). Therefore, the speed relation is used in the form of equation (11) evaluated at the sonic point,

$$\delta_*^2 = 1 - h\frac{M_*^2}{P_*^2}\left(H_* + \lambda_* Q\right). \tag{73}$$

where M_*, P_*, and H_* all retain the unsteady and curvature terms to $O(\dot{D},\kappa)$ and δ_*^2 is evaluated from the exact equation (33). Since $\delta_*^2 = O(\dot{n}_*^2)$, then $\dot{n}_*$ is absent in the speed relation to leading order and we can drop the left-hand side of equation (73) and hence obtain an equation that relates $\dot{D}$, D, and λ_* by expanding M_*, P_*, and H_*. Notice again, that

just like the compatibility condition the speed relation also does not contain $\dot{n}_*$ to the leading order, which leaves us with only two equations (instead of three in general) to solve for D and λ_*.

The correction terms M_{1*}, P_{1*}, and H_{1*}, found by substituting the quasi-steady planar solution, equations (13)-(16), into the integrands of equations (24)-(26), are

$$M_{1*} = -\dot{D} I_1 + \kappa D \left(n_{0*} - I_0\right), \tag{74}$$

$$P_{1*} = \dot{D} \left(n_{0*} - I_0\right) + \kappa D^2 \left(n_{0*} - J_0\right), \tag{75}$$

$$H_{1*} = -\dot{D} \left(n_{0*} - I_0 + \frac{1}{D} S_1\right), \tag{76}$$

where we denote various integrals as

$$n_{0*} = -D \int_0^{\lambda_{0*}} \frac{d\lambda_0}{\rho_0 \omega_0}, \quad I_0 = \int_0^{n_{0*}} \rho_0 dn, \quad J_0 = \int_0^{n_{0*}} v_0 dn, \tag{77}$$

$$I_1 = \int_0^{n_{0*}} \rho_{0D} dn, \quad S_1 = \int_0^{n_{0*}} p_{0D} dn. \tag{78}$$

The subscript D here denotes partial differentiation with respect to D. Note that n_{0*} is the leading-order position of the sonic locus. These integrals are calculated using the change of the integration variable $dn = -D v_0 d\lambda_0 / \omega_0$ and the upper limit of the integration to $\lambda_{0*} = 1 + F$.

Substituting $M_* = M_0 + M_{1*}$, $P_* = P_0 + P_{1*}$, $H_* = H_0 + H_{1*}$, with the corrections given by equations (74)-(76), into equation (73), we obtain after some algebra that the speed relation is given by

$$1 + F - \lambda_* + \kappa f + \dot{D} g = 0, \tag{79}$$

where we denote

$$f = \frac{2}{b^2} \left[n_{0*} - I_0 + \frac{D^2}{1 + D^2} \left(n_{0*} - J_0\right)\right], \tag{80}$$

$$g = \frac{2}{b^2} \left[\frac{1 + (1 + h/2) D^2}{\left(1 + D^2\right)^2} \left(n_{0*} - I_0\right) + \frac{hD}{2\left(1 + D^2\right)^2} S_1 - \frac{1}{D} I_1\right]. \tag{81}$$

In deriving (79), one takes advantage of the expansion $\lambda_* = \lambda_{0*} + \lambda_{1*}$ where $\lambda_{0*} = 1 + F = O(1)$ is the leading-order value of the progress variable at the sonic locus, and λ_{1*} is $o(1)$ correction to that. It is important to note that $F = O(1)$ and no assumption that $F = o(1)$ (that is $D - D_{CJ} = o(1)$) is necessary. Note also that the requirement that $\lambda_* \leq 1$ puts a constraint on F so that if detonation is overdriven, that is if $F > 0$, equation (79) may not have a solution for λ_*, which means that the sonic point may be absent in the flow.

We call equation (71) in which λ_* is substituted from the speed relation, equation (79), the *evolution equation*. In general, if higher-order terms are included, we have a system of evolution equations for D, λ_* and $\dot{n}_*$ comprised of the compatibility condition, the speed relation and also the rate equation evaluated to sufficiently high accuracy. The evolution equation, equation (71) admits a simple physical interpretation as the dynamical equation that governs the shock motion. It says that the shock acceleration is controlled by the competition between the heat release, represented by $a_1 \omega_*$, that tends to accelerate the shock, and the flow divergence $a_2 \kappa$ that takes the energy away from the shock and thus tends to decelerate it. The quasi-steady solution, $\dot{D} = 0$, corresponds to the exact balance of the two competing effects, $a_1 \omega_* = a_2 \kappa$, the equation that yields $D - \kappa$ relation.

IV. SOLUTIONS OF THE EVOLUTION EQUATION

Two equations, (71) and (79) are the main result of the present work. The evolution equation (71) is the $\dot{D} - D - \kappa$ relation that governs the dynamics of slowly-evolving weakly-curved detonations. The main purpose here is to use the equation for the analysis of detonation initiation and failure in the case of spherical or cylindrical detonations. But it is clear from the above derivations that the evolution equation (71) has wider applicability, namely to two-dimensional weakly-curved and slowly-varying detonations, as its derivation does not rely on specific spatial symmetry. Before proceeding to the analysis of solutions of the evolution equation we point out several of its general properties.

A. Properties of the evolution equation

Several comments should be made regarding the character of the $\dot{D} - D - \kappa$ relation derived above. Perhaps the most important feature of the relation is that its derivation does not require any *specific* assumptions about the ordering of either $D - D_{CJ}$ or $\dot{D}$ with regard to each other or κ. The only assumption is that of $\dot{D} = o(1)$ and $\kappa = o(1)$. The three quantities are related in the final result in a rather general form and involve a range of scales that would hardly be possible to anticipate *a priori*. As for any assumption for $D - D_{CJ}$, none is necessary to derive the above evolution equation.

There exists a dynamic change of the time scale in the evolution equation that can be seen from consideration of the near-CJ limit of $D - D_{CJ} = O(F)$, $F \to 0$. It is easy to see that two of the above integrals, namely I_1 and S_1 are in fact singular as $D \to D_{CJ}$ because of the derivatives of the seed state in the integrands. As shown in Appendix A, in the limit $F \to 0$ the integrals behave as follows

$$I_1 = \frac{constant}{|F|^{\nu-1/2}} + reg. \tag{82}$$

if $1/2 < \nu < 1$ and

$$I_1 = constant \, \ln|F| + reg. \tag{83}$$

if $\nu = 1/2$, where *reg* denotes regular terms. Integral S_1 has exactly similar behaviour. Since none of the other integrals except I_1 and S_1 are singular, we conclude that $\dot{D}$ changes its order, that is, it becomes smaller for near-CJ detonation compared to the dynamics with $D - D_{CJ} = O(1)$ by a factor of $O(|F|^{\nu-1/2})$. This is what we mean by "dynamic scale change" since the order of $\dot{D}$ is exactly the order of the time derivative. Hence near-CJ detonation in present theory evolves on a slower time scale than sub-CJ detonation.

The fact that the problem involves a range of scales, for example for near-CJ detonation can be seen from the evolution equation as follows. Suppose we assume *a priori* scales for $\kappa = O(\varepsilon)$ and $\partial_t = O(\varepsilon^\alpha)$, $\varepsilon \to 0$, $\alpha > 0$. The question is: What is the scale of $D - D_{CJ}$ that is consistent with the compatibility condition and the speed relation? Let $\kappa = \varepsilon\kappa'$ and $\dot{D} = \varepsilon^\alpha \dot{D}'$ with $\alpha \in (0,2)$ and $\kappa' = O(1)$, $\dot{D}' = O(1)$. Then equation (71) results in

$$1 - \lambda_* = O\left[(a_1\varepsilon + a_2\varepsilon^\alpha)^{1/\nu}\right] \tag{84}$$

while using the latter result, equation (79) gives

$$D - D_{CJ} = O\left[(a_1\varepsilon + a_2\varepsilon^\alpha)^{1/\nu}\right] - \varepsilon\kappa' f - \varepsilon^\alpha \dot{D}'. \tag{85}$$

From equation (85) we see immediately that a number of scales enters the expansion of $D - D_{CJ}$. For a more explicit example, take $\alpha = 3/2$ and $\nu = 3/4$. Then $1 - \lambda_* = O\left[\varepsilon^{1/\nu}\left(a_1 + a_2\varepsilon^{1/2}\right)^{1/\nu}\right] = O(\varepsilon^{1/\nu}) + O(\varepsilon^{1/\nu+1/2}) = O(\varepsilon^{4/3}) + O(\varepsilon^{11/6})$ and therefore

$$D - D_{CJ} = O(\varepsilon) + O(\varepsilon^{4/3}) + O(\varepsilon^{3/2}) + O(\varepsilon^{11/6}). \tag{86}$$

The last three terms are all intermediate between $O(\varepsilon)$ and $O(\varepsilon^2)$. Retaining them is essential for capturing the correct physics contained in the compatibility condition and the speed relation. Any *a priori* assignment of a single scale for $D-D_{CJ}$ in addition to those of κ and $\dot{D}$, although entirely legitimate, will produce an evolution equation which is restricted to phenomena on those scales only. But detonation with the sonic locus is intrinsically *multi-scale* phenomenon and in general requires treatment of all scales for capturing the correct dynamics. This shows that with pre-set scales of all the small quantities, one in general has to include a number of reaction-order dependent intermediate scales in the expansions of state variables.

An important conclusion from the above discussion is that in the present analysis we are looking at detonation dynamics that is subject to the distinguished limit that $\dot{D}\to 0$ as $D-D_{CJ}\to 0$. Clearly such a theory is insufficient for prediction of more complex dynamics such as pulsating or cellular detonations. Inclusion of higher-order terms with more accurate representation of the solution in the transonic layer (which is precisely the source of the singularities) avoids these difficulties as we discuss in the forthcoming paper (Kasimov & Stewart 2004).

Another observation concerns the magnitude of different terms in the evolution equation (71). The assumptions on which the theory is based are those of small time derivatives i.e. $\dot{D}=o(1)$ and small curvature, $\kappa=o(1)$. As a consequence of these assumptions and the compatibility condition (71) it follows that the reaction rate at the sonic locus must also be small, $\omega_*=o(1)$. By not specifying how exactly $\omega_*=o(1)$ the theory is general so that various asymptotic limits are included. The simplest example is $1-\lambda_*=o(1)$ with $D-D_{CJ}=o(1)$, which is consistent with $\omega_*=o(1)$. But $D-D_{CJ}=O(1)$ is included so long as $\omega_*=o(1)$. In the case if $\dot{D}=0$, then $\omega_*=O(\kappa)$ is all that is required when $D-D_{CJ}=O(1)$. That is the $D-\kappa$ curve is scaled by the reaction rate and lies in the neighbourhood of small curvature. In the special case of state-sensitive kinetics such as Arrhenius kinetics with large activation energy, ω_* is uniformly small as D decreases from D_{CJ} to the ambient sound speed, c_0.

We should also point out that the reaction mechanism is only assumed to be of one-step reaction described by a single progress variable. There has been no assumption made with regard to the form of the rate function. As far as mathematical character of the evolution equation, one can show that local linearization of the speed relation and the compatibility condition results in a hyperbolic partial differential equation provided the functions f and g are positive. One can easily prove that function f is always positive and numerical calculations show that function g is also positive.

B. Quasi-steady response: The $D-\kappa$ relation

Now let us calculate the quasi-steady $D-\kappa$ relation which is obtained by setting $\dot{D}=0$ in equation (71) for various parameter sets. We calculate $D-\kappa$ curves and analyze the effects of some of the constitutive parameters. Consider a gaseous explosive mixture with a rate law of Arrhenius form

$$\omega = k(1-\lambda)^{\nu}\exp\left(-\frac{E}{pv}\right). \tag{87}$$

Then, we find that to leading order

$$p_{0*}v_{0*}=c_{0*}^2/\gamma=\frac{1}{\gamma}\left(\frac{\gamma}{\gamma+1}\frac{1+D^2}{D}\right)^2 \tag{88}$$

and the evolution equation (71) becomes a $D-\kappa$ equation

$$F+\kappa f+\kappa^{1/\nu}\exp\left[\frac{\gamma E}{\nu}\left(\frac{\gamma+1}{\gamma}\frac{D}{1+D^2}\right)^2\right]\cdot\left[\left(\frac{\gamma}{\gamma+1}\right)^2\frac{(1+D^2)^2(D^2-\gamma)}{(\gamma^2-1)kQD^3}\right]^{1/\nu}=0. \tag{89}$$

We can immediately see that for $D-D_{CJ}=o(1)$ this is a familiar result (e.g. Klein and Stewart 1993), but importantly, equation (89) has no assumption in it regarding $D-D_{CJ}$ or the magnitude of the activation energy E.

Note that the general qualitative character of the $D-\kappa$ relation can be easily seen from the equation $a_1\omega_*=a_2\kappa$ as follows. Let us write the equation as

$$k(1-\lambda_*)^{\nu}\exp\left(-\frac{\gamma E}{c_*^2}\right)=\bar{a}(D-\sqrt{\gamma})\kappa. \tag{90}$$

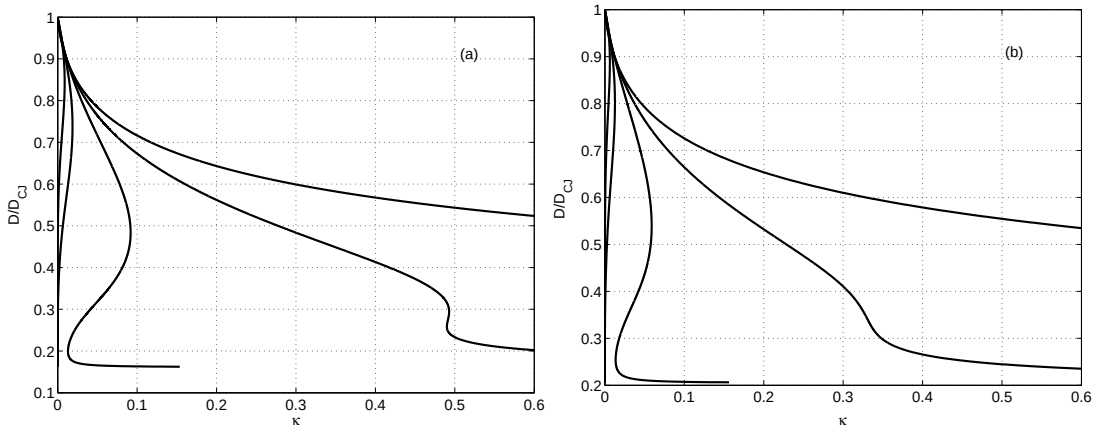

Figure 2: $D-\kappa$ curves for $\nu=1$, $\gamma=1.2$, $Q=50$ (a) and $Q=30$ (b) for various activation energies: $E=0,5,10,20$ and 30. E increases from right to left on each figure.

Now assume for simplicity that the speed relation yields $1-\lambda_*=-F=\bar{b}(D_{CJ}-D)$. Here we separate the important dependencies in a_1, a_2, and F by introducing $\bar{a}(D)$ and $\bar{b}(D)$ as certain weak functions of D. Then we obtain the following explicit formula for $\kappa(D)$:

$$\kappa=\bar{c}\frac{(D_{CJ}-D)^{\nu}}{D-\sqrt{\gamma}}\exp\left(-\bar{d}E/D^2\right), \tag{91}$$

where again $\bar{c}$ and $\bar{d}$ are weak functions of D. It is clear now from (91), that as D decreases below D_{CJ}, κ first increases from $\kappa=0$ because of the factor $(D_{CJ}-D)^{\nu}$, but then the exponential term that decreases as D goes down starts to dominate causing κ to decrease. As a result we have a first (upper) turning point at some $D=D_c$. The curvature will decrease after reaching the upper turning point until eventually D becomes close to the ambient sound speed, $\sqrt{\gamma}$, so that the denominator $D-\sqrt{\gamma}$ causes κ to grow again, which explains the existence of the second (lower) turning point. Since the exponential term although small, never vanishes, κ will eventually increase to infinity as $D\to\sqrt{\gamma}$. It is also clear that if the activation energy is sufficiently small, then the exponential term may not be able to compensate for the increase of κ due to $(D_{CJ}-D)^{\nu}$, in which case there will be no turning points and κ will increase monotonically to infinity. This simple picture explains the essential nature of the $D-\kappa$ relation that can exhibit two turning points.

Next we plot exact $D(\kappa)$ dependencies that follow from equation (89) for various values of E, Q, γ, and ν. Figure 2 shows $D-\kappa$ curves for varying activation energy for two different heat release parameters Q. Increasing activation energy from $E=0$, (in which case there are no turning points) to larger E causes two turning points appear, which move toward smaller κ as E is increased. Decreasing Q from $Q=50$ to $Q=30$ causes a similar change in $D-\kappa$ curves as does increasing the activation energy E.

Figure 3 shows variations of reaction order ν (a) and specific heat ratio γ (b). The reaction order is seen to have a negligible effect on the solution, except near the lower branch, where $\nu=3/4$ shows critical curvature larger than all other cases. Variations of the adiabatic exponent have much more significant effect on the $D-\kappa$ solution. The upper turning point is seen to move toward smaller curvature κ and larger velocity D as γ is decreased.

C. $\dot{D}-D-\kappa$ relation and the ignition/failure phenomenon

Next we apply the evolution equation (71) to describe the dynamics of a spherically expanding detonation wave in a mixture with heat release governed by the simple-depletion Arrhenius rate law

$$\omega=k(1-\lambda)\exp\left(-\frac{E}{pv}\right). \tag{92}$$

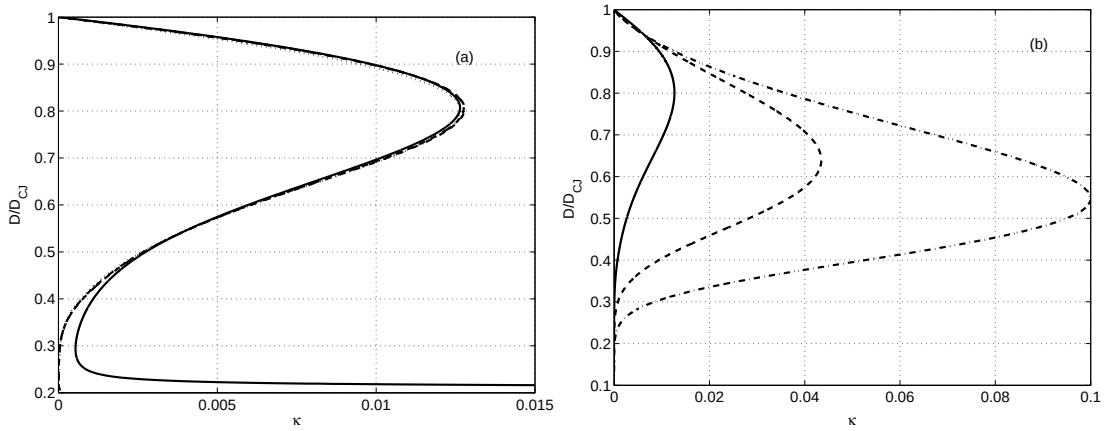

Figure 3: (a) $D-\kappa$ curves for $\gamma = 1.2$, $Q = 30$, $E = 20$ for several reaction orders, $\nu = 1/2$ (solid), $\nu = 2/3$ (dashed), $\nu = 3/4$ (dash-dot), and $\nu = 1$ (dotted); (b) $D-\kappa$ curves for $\nu = 1$, $Q = 30$, $E = 20$ for several γ: $\gamma = 1.2$ (solid), $\gamma = 1.4$ (dashed), and $\gamma = 1.6$ (dash-dot).

We write the evolution equation as a second-order ordinary differential equation in the shock radius $R = 2/\kappa$, $D = \dot{R}$, and $\dot{D} = \ddot{R}$. Our goal is to obtain the solution of the equation subject to the initial conditions, $\dot{R}(0) = D_0$ and $R(0) = R_0$ for different values of D_0 and R_0. As a specific example, we consider a mixture with $\gamma = 1.25$, $Q = E = 40$, which is representative of near-stoichiometric hydrogen-oxygen mixtures.

The quasi-steady response curve for this parameter set is shown in figure 4(a) with the upper turning point at $\kappa_c = 7.19 \cdot 10^{-3}$, $D_c/D_{CJ} = 0.876$, where $D_{CJ} = 6.8896$. The lower turning point is located at essentially zero curvature (less than 10^{-8}). Figure 4(b) demonstrates the ignition and failure phenomenon exhibited by the evolution equation. Equation (71) is solved starting from variety of initial conditions, which are chosen so that $R_0 = 200$ is fixed and D_0 is varied from about CJ value 6.8 to 5.0. If D_0 is sufficiently large, then the shock speed first decays to a certain minimum, which is reached at the quasi-steady curve, $\dot{D} = 0$, and then increases, asymptotically approaching the quasi-steady $D-R$ curve as $R \to \infty$. In this case we have a successful initiation. If the initial shock speed is sufficiently low, then the solution has a qualitatively different character, namely the shock speed continues to decay and does not recover until very large distances are reached, that correspond to the lower turning point in figure 4(a), so that the distance is at least $2 \cdot 10^8$. As the solution crosses the lower branch, the shock acceleration $\dot{D}$ becomes positive and ignition results. As figure 2 shows, the curvature at the lower turning point decreases rapidly with increasing activation energy, thus the re-ignition of the initially failed detonation will take place at very large distances for sufficiently large activation energies, which are typical of real mixtures, and thus can be essentially ignored. The existence of the lower turning point is a feature of the one-step Arrhenius kinetics, that allows for a finite reaction rate at arbitrarily low shock speeds (hence shock temperatures). In reality, the chemical reactions responsible for the heat release may terminate if the gas temperature drops below a certain, mixture dependent value. Extensions of the theory to include more complex chemistry that includes such property of the realistic chemistry should eliminate the re-ignition behaviour associated with the lower turning point. We should emphasize that the essential mechanism of the initiation/failure phenomenon is principally associated with the upper turning point, which is expected to exist for arbitrary chemistry models. Thus, despite its simplicity the Arrhenius kinetics is still capable of describing the main physical mechanism of the initiation process.

The dash-dot line in figure 4(b) is what we call an *ignition separatrix*. It is a curve $D_{IS}(R)$ that delineates initial conditions that lead to ignition (above the curve) and those that lead to failure (below the curve). One can easily calculate the ignition separatrix by taking the initial condition at sufficiently large R and just below the middle branch of the $D-R$ curve and integrating the evolution equation (71), backward in time.

The solution that starts just above the separatrix, that is at $D_0 = 5.85$ most clearly shows that between the initial decay and final acceleration of the shock there is a relatively long phase of almost constant shock speed. Similar behaviour is also observed in both numerical simulations and experiments, and the phase has been called "a quasi-steady" stage of detonation initiation (e.g. Lee & Higgins 1999). The term may be justified to some degree as the detonation does indeed have very small acceleration (none exactly at the lower branch of the quasi-steady $D-R$ curve), the acceleration, however small, is followed by a very rapid approach to the CJ velocity. The closer the initial

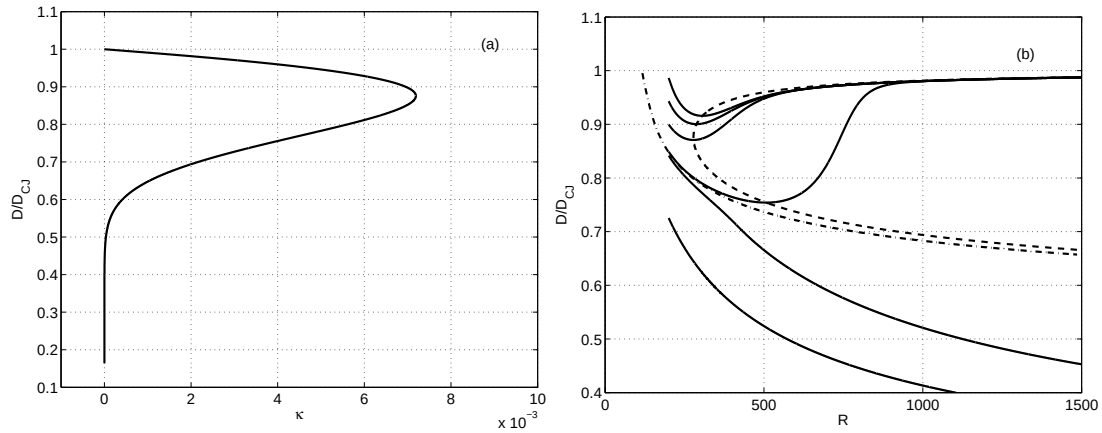

Figure 4: (a) $D-\kappa$ curve for detonation in an ideal gas with $\gamma = 1.25$, $Q = E = 40$; (b) Ignition and failure. Dashed line is the quasi-steady $D-R$ curve, dash-dot line is the ignition separatrix, and solid lines are solutions of equation (71) with initial conditions given by $R_0 = 200$ and various D_0, $D_0 = 6.8$, 6.5, 6.2, 5.85, 5.84, and 5.0 from top to bottom.

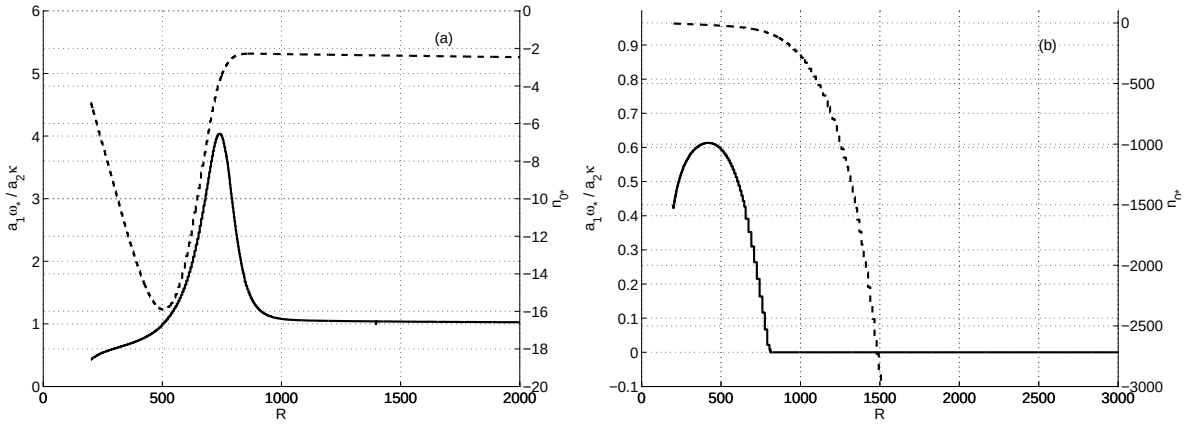

Figure 5: Position of the sonic locus, n_{0*} and the ratio of the heat release term $a_1\omega_*$ to the curvature term $a_2\kappa$ in equation (71) during successful ignition (a) and failure (b) for detonation in an ideal gas with $\gamma = 1.25$, $Q = E = 40$. (a) corresponds to $R_0 = 200$, $D_0 = 5.85$, (b) corresponds to $R_0 = 200$, $D_0 = 5.841$.

condition to the ignition separatrix, the more extended the "quasi-steady" stage is.

Figure 5 shows plots of the ratio of the heat release, $a_1\omega_*$ and curvature (or divergence), $a_2\kappa$ terms in equation (71) and the location of the sonic locus, n_{0*} during ignition (a) and failure (b). In the case of the successful initiation, (a), one can see that $a_1\omega_*/a_2\kappa$ is less than unity, hence $\dot{D} < 0$ during the initial decay of the shock (see equation 71), and until its value reaches unity, the sonic locus retreats from the shock. As the ratio $a_1\omega_*/a_2\kappa$ becomes equal to unity and starts increasing further, the sonic locus reverses its direction and starts moving toward the shock. There is a rapid increase of the heat release term during the initiation phase, and then the term decreases because of the fuel depletion at the sonic locus, that is because $\lambda_* \to 1$. As R further increases, both the reaction term $a_1\omega_*$ and curvature term $a_2\kappa$ tend to zero, their ratio approaching unity, and hence $\dot{D}$ approaching zero. The failed case is shown in figure 5(b), where the reaction term $a_1\omega_*$ is seen to remain much smaller than the curvature term and the sonic locus keeps retreating from the lead shock. Therefore, the dominating flow divergence, $a_2\kappa$ in this case results in detonation failure.

D. The direct initiation and critical energy

Criticality of solutions of the evolution equation, equations (71), demonstrated in figure 4 is a function of the initial conditions, D_0 and R_0. Importantly, the mechanism by which the initial condition is created can be arbitrary and depends on specific means of initiating the detonation. One important means is by direct initiation by a blast release of concentrated energy. Direct initiation can be accomplished by a hypervelocity projectile and detonation re-initiation upon diffraction round a corner. Diffracted detonation wave may fail in certain cases and identification of the failure conditions has implications for the problem of detonation transmission from confined into unconfined space. The failure can be predicted by the above theory provided the initial conditions from the early stage of the diffracted detonation correspond to detonation radius and speed below those of the ignition separatrix. Such calculations of detonation diffraction and comparisons with the present theory are being carried out in our group by B. Wescott and will be reported on shortly.

We now give more details on how the direct initiation can be treated using the present theory. The main idea is to relate the characteristics of the strong blast wave such as its shock speed, D_{bw} and radius, R to the initial conditions, D_0 and R_0 required to solve the evolution equation. If the energy of the blast wave, E_{bw} is sufficiently large so that the point (R, D_{bw}) happens to be above the ignition separatrix at some point of the blast-wave decay, then successful ignition would follow. Otherwise, the blast wave would continue to decay and consequently lead to detonation failure. Then, a critical energy, E_c exists such that the decaying blast wave follows the ignition separatrix. Thus, given the strong-blast wave solution, we can identify its strength that would correspond to the ignition separatrix. A simple way to estimate the critical energy is to require that the blast-wave solution and the ignition separatrix match at, for example, $D = D_{CJ}$. Let us denote the corresponding radius on the ignition separatrix as R_s. Then we obtain the criticality condition

$$D_{bw}(R_s, E_c) = D_{CJ}. \tag{93}$$

The blast-wave solution $D_{bw}(R, E_{bw})$ depends parametrically on the blast energy E_{bw}, thus allowing us to extract the critical energy from equation (93).

In the case of a detonation with point symmetry ($j = 0, 1, 2$ correspond to planar, cylindrical and spherical symmetry, respectively) one can use Korobeinikov's extension of the Taylor-Sedov blast-wave formula (Korobeinikov 1991; Eckett *et al.* 2000),

$$E_{bw} = A_j \left(\frac{j+3}{2} \right)^2 \rho_0 D_{bw}^2 R^{j+1} \exp\left(-\frac{B_j Q}{D_{bw}^2} \right), \tag{94}$$

which accounts for the leading-order asymptotic effect of the chemical reaction on the strong blast dynamics. In the case of a spherical detonation, the constants A_2 and B_2 are functions of γ that can be calculated by the following formulas,

$$A_2 = 0.31246\,(\gamma-1)^{-1.1409-0.11735\log_{10}(\gamma-1)}, \tag{95}$$

$$B_2 = 4.1263\,(\gamma-1)^{1.253+0.14936\log_{10}(\gamma-1)}, \tag{96}$$

which are valid for $1.2 \le \gamma \le 2$. For the parameter set that we used to plot figure 4, that is $\gamma = 1.25$, $Q = E = 40$, we find that $R_s = 114.6$, $D_{CJ} = 6.8896$, and the critical energy $E_c = 3.08 \cdot 10^8$.

If one has thermodynamic and kinetic data that describe real mixtures within the framework of the ideal-gas equation of state and one-step Arrhenius kinetics, one can follow the above procedure to estimate the critical energies for real mixtures. Such thermo-chemical data obtained from detailed chemical calculations of the steady one-dimensional detonations (e.g. the activation energy E, heat release Q, von Neumann temperature, reaction zone lengths, etc.) can be found at Caltech detonation database (Kaneshige *et al.* 1997). As for the adiabatic exponent γ which is assumed constant and the same for the reactants and products, one can obtain it from the shock conditions by demanding that the shock temperature agrees with detailed numerical predictions. Therefore, from the detailed chemical calculations we retain the effective activation energy, the total heat release, and the von Neumann temperature, all of which are of the most significance for the detonation dynamics. Figure 6 shows comparison of the critical energies calculated by

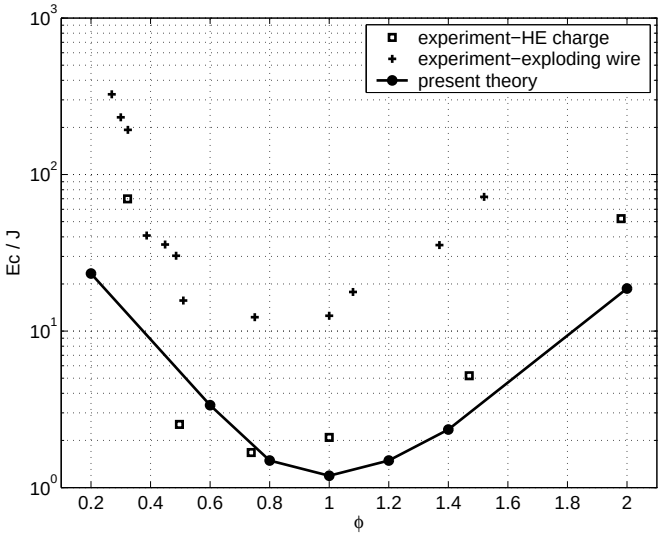

Figure 6: Comparison of theoretical critical initiation energy for $H_2 - O_2$ mixtures of various equivalence ratios ϕ with experiments (HE initiation - Matsui & Lee 1979; exploding bridge-wire - Litchfield *et al.* 1962).

this method for $H_2 - O_2$ mixtures of various equivalence ratios ϕ against experimental data (which are again found at the Caltech detonation database).

Two sets of experimental data are plotted, which correspond to different means of strong initiation, namely by a high explosive discharge and an exploding bridge-wire. For calculations of the dimensional critical energies one also needs to know the dimensional half-reaction length $\tilde{l}_{1/2}$. We took $\tilde{l}_{1/2}$ equal to the reaction zone lengths found at Caltech database, which are based on a detailed chemical mechanism and correspond to the distance from the shock to the point in the reaction zone at which the temperature gradient attains a maximum. While this may not exactly be the half-reaction length, they are sufficiently close for our purpose here. One can see that despite the simplicity of the underlying constitutive description, the agreement of the theory and experiment, in particular the one with high-explosive initiation, is remarkably good. The experiment with high-explosive (HE) initiation compares better with present theory because the blast wave formed due to HE detonation is more likely to represent a point explosion than the wave formed in the exploding bridge-wire experiment. Experimental results on direct initiation are themselves subject to often more than an order of magnitude difference and the comparison should be looked at with that caveat in mind. In addition, simplicity of chemistry employed by the theory may have consequences. But more careful studies of the initiation are required in all respects before a more definitive conclusion can be reached (for further discussion see also Eckett *et al.* 2000).

To summarize the critical energy calculation procedure, given the mixture global thermo-chemical parameters such as γ, Q, ν, and E, we can compute the ignition separatrix by solving the evolution equation (71), and find R_s, then find the critical initiation energy E_c from equations (93)-(96).

E. On weak initiation

Now we consider initiation by a weak source that can also be treated with present theory. While the theory of direct (strong) initiation discussed in the preceding section is closely related to the properties of the $D - \kappa$ curve near the upper turning point, weak initiation has to do with the lower turning point. Note that if one looks at the sign of $\dot{D}$ at different regions of $D - R$ plane, one finds that to the left of the quasi-steady $D - R$ curve, the acceleration is negative, that is $\dot{D} < 0$, while to the right it is positive. Consequently, below the lowest branch of the quasi-steady $D - R$ curve (see figure 7), at shock speeds very near the ambient sonic speed, the shock acceleration is positive, and therefore ignition from such initial conditions is possible.

In figure 7, we consider detonation in a gas with $\gamma = 1.2$, $Q = 50$, $\nu = 1$, and activation energy $E = 13$ which is sufficiently small so that the lower turning point is not at unreasonably large distances. If we solve the evolution

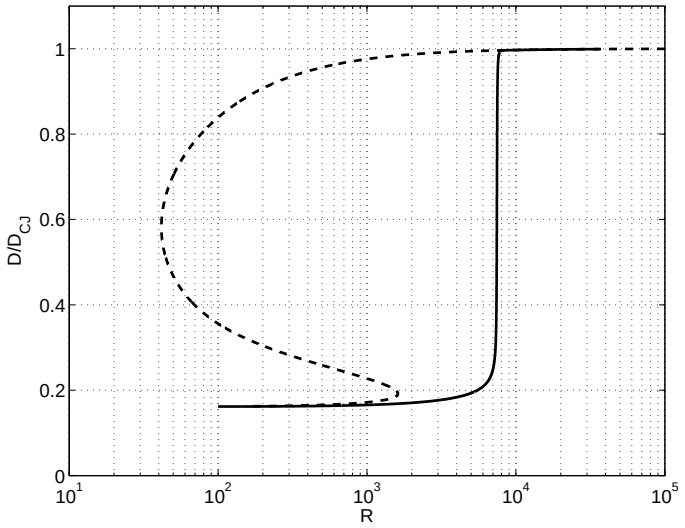

Figure 7: Detonation initiation by a weak source for a mixture with $\gamma = 1.2$, $Q = 50$, $E = 13$. Solid line is a quasi-steady $D-R$ curve and dashed line is a solution of the $\dot{D}-D-\kappa$ equation with initial conditions $D_0 = 1.101$, $R_0 = 100$.

equation (71) starting from an initial condition just below the quasi-steady curve, at $D_0 = 1.101$ and $R_0 = 100$, then the detonation evolves so that the solution $D(R)$ remains below the quasi-steady curve until it passes the lower turning point, after which the shock speed starts to increase rapidly, indicating transition to the CJ detonation.

It is interesting to look at the position of the sonic locus as it varies with the shock speed. Figure 8(a) shows how the sonic locus defined as

$$n_{0*} = -D\int_0^{1+F} \frac{d\lambda_0}{\rho_0\omega_0} = -D\int_0^{1+F} \frac{\exp\left(\gamma E/c_0^2\right)d\lambda_0}{\rho_0 k(1-\lambda_0)} \tag{97}$$

varies along the quasi-steady $D-R$ curve of figure 7. One can see that along both upper and lower stable branches of $D-R$ curve, the sonic locus tends to be much closer to the shock than along the middle branch, which implies that both near-CJ detonation (F close to 0) and near-sonic detonation (F close to -1) have small domains of influence with sonic locus near the lead shock. The situation for the unstable middle branch of $D-R$ curve is different. The sonic locus for such detonation can move away from the shock to very large distances. This behaviour follows from the definition (97). If F is close to 0, then c_0^2 (which is proportional to the temperature in the reaction zone) is sufficiently large so that the exponential in the integrand is not a large quantity. If on the other hand, we look at the middle branch, the post-shock temperature drops so much that the exponential is a large number with a consequence that the sonic locus moves further from the shock. The reason that the sonic locus returns closer to the shock as we get close to the bottom branch of the $D-R$ curve is that as $D \to c_a = \sqrt{\gamma}$, we get $F \to -1$, and so the upper limit of the integration in (97) tends to 0. Figure 8(b) show how the sonic locus evolves during the weak initiation shown in figure 7.

This phenomenon of weak initiation could in principle be related to any initiation mechanism that creates the initial condition such that the detonation is very slightly supersonic. For example, in the case shown in figure 7, the initial detonation Mach number is $D_0/\sqrt{\gamma} = 1.005$. Here we do not discuss in any detail possible physical situations that could result in such initial conditions, but clearly one can think of many (e.g. weak shocks that can arise in the deflagration-to-detonation transition). We also note that of course, if the initial condition is just above the quasi-steady curve, one would still obtain ignition after the solution passes through the neighbourhood of the lower turning point of the quasi-steady $D-R$ curve.

If the activation energy is sufficiently large, then the weak initiation becomes problematic as the lower turning point moves to very large distances. In such cases, a sufficiently strong shock must be created such that the initial condition corresponds to states well above the lower branch of the quasi-steady $D-R$ curve if successful initiation is to be expected.

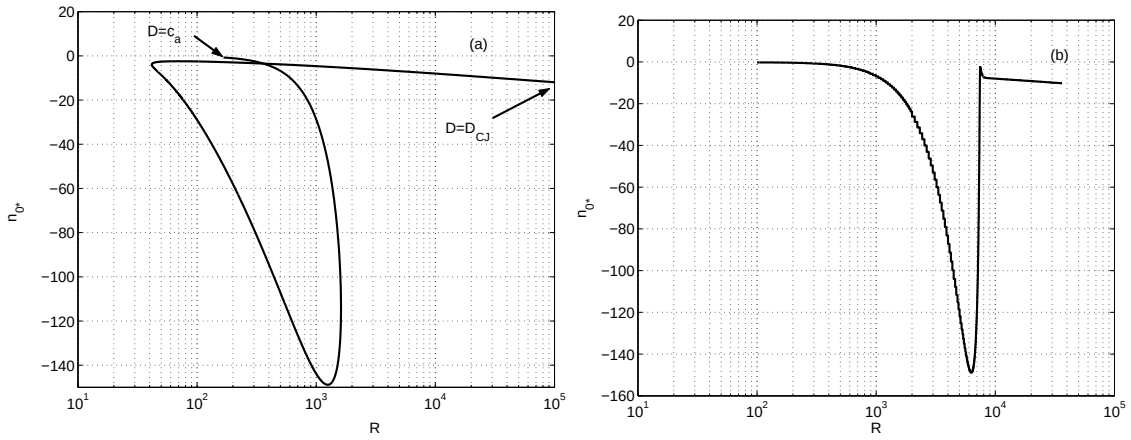

Figure 8: (a) The sonic locus along the quasi-steady $D-R$ curve and (b) the sonic locus for weak ignition, both of figure 7.

V. LARGE-ACTIVATION-ENERGY FORM OF THE EVOLUTION EQUATION

All integrals in the evolution equation are of the form

$$G = \int_0^{1+F} g(\lambda, D)\frac{d\lambda}{\omega}. \tag{98}$$

In the limit of large activation energy, the integral can be simplified and can be calculated explicitly. Let us write

$$\omega = k(1-\lambda)^{\nu}\exp(-\vartheta)\exp\left[\vartheta\left(1-\frac{c_s^2}{c_0^2}\right)\right], \tag{99}$$

where c_s^2 is the sound speed at the shock and $\vartheta = \gamma E/c_s^2$ is the activation energy, that we consider to be large, that is we compute the integrals in the asymptotic limit of large ϑ. Since $c_0^2/c_s^2 = T/T_s$ and the temperature at the shock is lowest within the reaction zone, the largest contribution to the integral comes from near the shock, that is from the induction zone.

Since

$$p_0 = \frac{1+D^2}{\gamma+1}(1+\gamma\delta_0), \quad v_0 = \frac{\gamma}{\gamma+1}\frac{D^2}{1+D^2}(1-\delta_0), \tag{100}$$

and $\delta_0 = b\sqrt{1+F-\lambda_0}$, we find

$$c_0^2 = c_*^2(1+\gamma\delta_0)(1-\delta_0). \tag{101}$$

Here $c_*$is the sound speed at the sonic point. Now let $s = \lambda/(1+F)$ and expand c^2in small s:

$$c_0^2 = c_*^2\left(\alpha_1+\alpha_2 s+O(s^2)\right) = c_s^2(1+\beta s)+O(s^2), \tag{102}$$

where

$$\beta = \frac{\gamma b_1^2-(\gamma-1)b_1/2}{1+(\gamma-1)b_1-\gamma b_1^2}, \tag{103}$$

and $b_1 = b\sqrt{1+F}$. Then

$$\frac{c_s^2}{c_0^2} = 1 - \beta s + O(s^2). \tag{104}$$

Using this expansion we find that

$$G \sim g(0,F)\frac{1+F}{k\beta}\frac{\exp(\vartheta)}{\vartheta}. \tag{105}$$

Define

$$\Phi = \frac{1+F}{k\beta}\frac{\exp(\vartheta)}{\vartheta}. \tag{106}$$

Then the integrals n_{0*}, I_0, and J_0 in the $D-\kappa$ equation are

$$n_{0*} = -D\int_0^{1+F}\frac{d\lambda_0}{\rho_0\omega_0} = -Dv_s\Phi, \tag{107}$$

$$I_0 = -D\int_0^{1+F}\frac{d\lambda_0}{\omega_0} = -D\Phi, \quad J_0 = -D\int_0^{1+F}\frac{d\lambda_0}{\rho_0^2\omega_0} = -Dv_s^2\Phi. \tag{108}$$

The function f becomes

$$f = \frac{2}{b^2}D\Phi(1-v_s)\left[1 - \frac{D^2}{1+D^2}v_s\right] = f_0\Phi. \tag{109}$$

This asymptotic form exhibits the $D-\kappa$ curve very nicely.

Similarly, integrals I_1 and S_1 in g are

$$I_1 = -D\int_0^{1+F}(\ln\rho_0)_D\frac{d\lambda_0}{\omega_0} = -D\left(\frac{\rho_{0D}}{\rho_0}\right)_s\Phi, \tag{110}$$

$$S_1 = -D\int_0^{1+F}\frac{p_{0D}}{\rho_0}\frac{d\lambda_0}{\omega_0} = -D\left(\frac{p_{0D}}{\rho_0}\right)_s\Phi. \tag{111}$$

It is assumed that $F < 0$, that is sub-CJ detonations are considered. The derivatives of p_0 and ρ_0 are

$$(\ln\rho_0)_D = -(\ln v_0)_D = \frac{2}{D(1+D^2)} + \frac{1}{1-\delta_0}\delta_{0D}, \tag{112}$$

$$\frac{p_{0D}}{\rho_0} = \frac{c_0^2}{\gamma}(\ln p_0)_D = \frac{c_0^2}{\gamma}\left[\frac{2D}{1+D^2} + \frac{\gamma}{1+\gamma\delta_0}\delta_{0D}\right]. \tag{113}$$

And

$$\delta_{0D} = b_D\sqrt{1+F-\lambda_0} + \frac{b}{2}\frac{F_D}{\sqrt{1+F-\lambda_0}}, \tag{114}$$

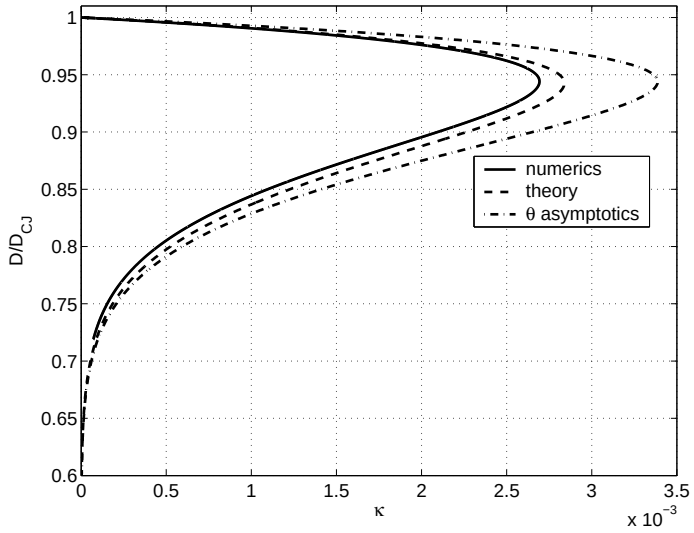

Figure 9: Comparison of the exact theory, large ϑ asymptotic version of the theory, and numerically computed $D-\kappa$ curves for $\gamma=1.2$, $E=50$, and $Q=30$.

$$b_D=\frac{D_{CJ}^2-\gamma}{\gamma D_{CJ}}\frac{1-D^2}{\left(1+D^2\right)^2},\quad F_D=\frac{2D_{CJ}^2\left(D^4-\gamma^2\right)}{D^3\left(D_{CJ}^2-\gamma\right)^2}. \tag{115}$$

$$g=g_0\Phi. \tag{116}$$

Figure 9 shows comparisons of the exact theory, large ϑ asymptotic version of it and the direct numerical solution of the reduced Euler equations (19)-(22), with no unsteady terms. The algorithm for the numerical $D-\kappa$ curve that we used to produce figure 9 is explained in Appendix B. One can see a remarkable agreement between the present theory and numerically generated $D-\kappa$ solution for the entire curve from D_{CJ} down to the lower turning point.

VI. CONCLUSIONS

In this paper we have presented a simplified version of a general theory developed by us (Kasimov 2004, Stewart & Kasimov 2004) that treats detonation waves with an embedded sonic locus in the asymptotic limit of small curvature and slow-time variation, and applied the theory to the problem of initiation of spherical/cylindrical detonation. We derived a front evolution equation that is a relationship between the shock acceleration, shock speed, and the local shock curvature. Solutions of the equation are shown to exhibit ignition/failure phenomenon. An important property of the equation is that it predicts criticality and identifies an ignition separatrix which is a curve in the plane of the shock speed versus the shock radius such that any initial condition on one side of it leads to ignition while that on the other side to failure.

The theory is developed based only on the assumptions of slow time variation, weak curvature, and negligible transverse variations at the shock front, and is valid for shock speeds that can deviate from CJ speed by $O(1)$ amount. A more general version of the theory that includes higher-order time and curvature effects is developed in Kasimov & Stewart (2004), but the present simplified version is capable of capturing the essential critical behaviour of the detonation dynamics. Finer details of the initiation process such as the front oscillations observed in numerical simulations and experiments must be treated with a higher-order theory. Clearly, the present theory can predict the ignition and failure only for curved detonations. Yet, one-dimensional planar detonations also exhibit critical behaviour. For their prediction the theory also needs to be extended to include higher order unsteady effects, as they are likely to be responsible for the criticality in planar geometry.

Other prospects of the present approach include the analysis of ignition in an explosive with more complex constitutive description. An extension of the theory to non-ideal equation of state is of much practical interest, for example in relation to detonation initiation in high explosives. Most of the calculations will then have to be done numerically, but in principle, the compatibility condition and the speed relation can be formulated without difficulty. This work in collaboration with Wescott will be reported in a sequel to the paper. Of equal importance is the extension to more complex kinetics. Chain-branching kinetics or kinetics with endothermic reactions may all play a role in detonation initiation and require further investigation with careful comparison against numerics and extensive experimental data available today.

Acknowledgments

This work was financially supported by U.S. Air Force Office of Scientific Research under contracts F49620-00-1-0005 and F49620-03-1-0048 (Program Manager Dr. Arje Nachman). D.S.S. was also supported by the U.S. Air Force Research Laboratory Munitions Directorate, Eglin AFB, under contract F8630-00-1-0002, and by the U.S. Department of Energy, Los Alamos National Laboratory, DOE/LANL 3223501019Z.

Appendix A: ASYMPTOTICS OF I_1 AND S_1 AS $D \to D_{CJ}$

Let us calculate the singular terms in I_1 and S_1. Since both p_0 and ρ_0 depend on δ_0 then their derivatives will depend on δ_{0D} which produces the derivative of $\sqrt{1+F-\lambda_0}$. In the limit $F \to 0$, the integrands in I_1 and S_1 have terms proportional to

$$\frac{1}{\sqrt{1+F-\lambda_0}\,(1-\lambda_0)^{\nu}} \tag{A1}$$

which are sources of singular behaviour if $\nu \geq 1/2$. Note, that if $\nu < 1/2$ the integrals are regular.

We have

$$p_{0D} = \frac{\gamma}{\gamma+1}\left(1+D^2\right)\frac{bF_D}{2}\frac{1}{\sqrt{1+F-\lambda_0}} + reg., \tag{A2}$$

$$\left(\ln\rho_0\right)_D = \frac{1}{1-\delta_0}\frac{bF_D}{2}\frac{1}{\sqrt{1+F-\lambda_0}} + reg., \tag{A3}$$

where *reg* denotes regular terms. Then

$$I_1 = -D\int_0^{\lambda_{0*}} \frac{1}{1-\delta_0}\frac{bF_D}{2}\frac{1}{\sqrt{1+F-\lambda_0}}\frac{d\lambda_0}{\omega_0} + reg. = -\frac{DbF_D}{2k}\int_0^{\lambda_{0*}} \frac{1}{1-\delta_0}\frac{\exp\left(\gamma E/c_0^2\right)}{\sqrt{1+F-\lambda_0}}\frac{d\lambda_0}{(1-\lambda_0)^{\nu}} + reg. \tag{A4}$$

Let $F \to 0_-$ in which case $\lambda_{0*} = 1+F$. Let $y = \sqrt{1+F-\lambda_0}$ and then denoting the integral in (A4) as I_{1s} we find

$$I_{1s} = \frac{2}{(-F)^{\nu}}\int_0^{\sqrt{1+F}} \frac{dy}{1-by}\frac{\exp\left(\gamma E/c_0^2\right)}{\left(1-y^2/F\right)^{\nu}} = \frac{2}{(-F)^{\nu}}\int_0^{\sqrt{1+F}} \frac{dy}{1-by}\exp\left(-\nu\ln\left(1-y^2/F\right)+\gamma E/c_0^2\right). \tag{A5}$$

Since $F \to 0$, the main contribution to the integral comes from $y \to 0$. We expand the logarithm in small y^2/F and obtain

$$I_{1s}=\frac{2}{(-F)^{\nu}}\int_0^{\sqrt{1+F}}\frac{dy}{1-by}\exp\left(\nu y^2/F+\gamma E/c_0^2+O\left(y^4/F^2\right)\right)\sim\frac{\exp\left(\gamma E/c_{0*}^2\right)}{(-F)^{\nu}}\sqrt{-\frac{\pi F}{\nu}}\,, \tag{A6}$$

and therefore

$$I_1=-\frac{DbF_D}{2k}\sqrt{\frac{\pi}{\nu}}\exp\left(\gamma E/c_{0*}^2\right)\frac{1}{(-F)^{\nu-1/2}}+reg.,\quad F\to 0_-. \tag{A7}$$

If $\nu=1/2$, a logarithmic singularity in (A5) appears. Indeed, by letting $y=\xi\sqrt{-F}$ in (A5), we find

$$I_{1s}=2\int_0^{\xi_*}\frac{d\xi}{1-by}\frac{\exp\left(\gamma E/c_0^2\right)}{\sqrt{1+\xi^2}}\sim-2\frac{\exp\left(\gamma E/c_{0s}^2\right)}{1-b}\ln\left(\xi_*\right), \tag{A8}$$

where $\xi_*=\sqrt{-\left(1+F\right)/F}\to\infty$. Therefore

$$I_{1s}=-\frac{2\exp\left(\gamma E/c_{0s}^2\right)}{1-b}\ln\left(-F\right). \tag{A9}$$

Subscript s here indicates evaluation at the shock, that is at $\lambda_0=0$.

Calculation of the second integral, S_1, is quite similar and yields the same singular behaviour as for I_1, that is again

$$S_1\sim\frac{constant}{|F|^{\nu-1/2}}+reg. \tag{A10}$$

or a logarithmic singularity if $\nu=1/2$.

Appendix B: ON NUMERICAL CALCULATION OF THE $D-\kappa$ RELATION

One writes the quasi-steady system of mass and momentum equations as

$$M_\lambda=-\kappa\phi, \tag{B1}$$
$$P_\lambda=-\kappa\phi U, \tag{B2}$$

where

$$\phi=\frac{M\left(U+D\right)}{\omega\left(p,v,\lambda\right)}, \tag{B3}$$

and

$$U=Mv,\quad p=P-M^2v, \tag{B4}$$

$$v=\frac{\gamma}{\gamma+1}\frac{P}{M^2}\left[1-\sqrt{1-h\frac{M^2}{P^2}\left(H_0+Q\lambda\right)}\right]. \tag{B5}$$

Now the thermicity condition can be written as

$$\kappa U_*^2 (U_* + D) - (\gamma - 1) Q \omega_* = 0, \tag{B6}$$

where, for Arrhenius kinetics,

$$\omega_* = k (1 - \lambda_*)^\nu \exp\left(-\frac{\gamma E}{U_*^2} \right) \tag{B7}$$

becomes a function of U_* only if we take advantage of the energy equation which can directly be integrated and takes a simple form, $H_* = H_0 = \gamma/(\gamma - 1) + D^2/2$, that is

$$\frac{\gamma + 1}{2(\gamma - 1)} U_*^2 - \lambda_* Q = H_0, \tag{B8}$$

so that

$$\lambda_* = \frac{1}{Q} \left(\frac{\gamma + 1}{2(\gamma - 1)} U_*^2 - H_0 \right). \tag{B9}$$

The sonic condition to be used for iterations on κ is

$$P_*^2 - h M_*^2 (H_0 + \lambda_* Q) = 0. \tag{B10}$$

Thus the numerical procedure is as follows. Given D, one solves (B10) for κ by iterations. At each iteration step, knowing a guess for κ, one solves (B1) and (B2) from the shock, using RH conditions, $M_0 = -D$ and $P_0 = 1 + D^2$ to $\lambda = \lambda_*$, where λ_* is found from the system of two algebraic equations, (B9) and (B6), for λ_* and U_*. Then, κ is varied in the iteration procedure until equation (B10) is satisfied to prescribed accuracy. After κ is found, D is decreased by a given decrement, and the procedure is repeated to find a new κ. Arclength continuation can be used for faster integration, but simple scanning of D with subsequent solution for κ works reasonably well.

---

[1] Aslam, T. D., Bdzil, J. D. & Stewart, D. S. 1995 Level-set methods applied to modelling detonation shock dynamics. *J. Comput. Phys.* **126**, 390-409.

[2] Aslam, T. D., Bdzil, J. B. & Hill, L. G. 1998 Extensions to DSD theory: Analysis of PBX9502 rate stick data. In *Eleventh Symposium (Intl) on Detonation*. Office of Naval Research, 21-29.

[3] Bdzil, J. B. 1981 Steady-state two-dimensional detonation. *J. Fluid Mech.* **108**, 185-286.

[4] Bdzil, J. D. & Stewart, D. S. 1989 Modelling of two-dimensional detonation with detonation shock dynamics. *Phys. Fluids A*, **1**, 1261-1267.

[5] Benedick, W. B., Guirao, C. M., Knystautas, R. & Lee, J. H. S. 1986 Critical charge for the direct initiation of detonation in gaseous fuel-air mixtures. In Bowen, J. R., Leyer, J.-C. & Soloukhin, R. I. (Eds.), *Prog. Astronaut. Aeronaut.* **106**, 181-202.

[6] Eckett, C. A., Quirk J. J. & Shepherd, J. E. 2000 The role of unsteadiness in direct initiation of gaseous detonations. *J. Fluid Mech*. **421**, 147-183.

[7] Eyring, H., Powell, R. E., Duffy, G. H. & Parlin, R. B., 1949 The stability of detonation. *Chem. Rev.* **45**, 69-181.

[8] Fickett, W. & Davis, W. C. 1979 *Detonation*, University of California Press.

[9] He, L. & Clavin, P. 1994 On the direct initiation of gaseous detonations by an energy source. *J. Fluid Mech.* **277**, 227-248.

[10] Kaneshige, M., Shepherd, J. E. & Teodorczyk, A. 1997 Detonation database at *Explosion Dynamics Laboratory*, Caltech, http://www.galcit.caltech.edu/EDL/.

[11] Kasimov, A. R. 2004 On the stability and nonlinear dynamics of detonation waves. PhD thesis, Theoretical and Applied Mechanics, University of Illinois at Urbana-Champaign.

[12] Kasimov, A. R. & Stewart, D. S. 2003 On the dynamics of self-sustained one-dimensional detonations: A numerical study in the shock-attached frame. TAM Report No. 1035, TAM, University of Illinois.

[13] Kasimov, A. R. & Stewart, D. S. 2004 Asymptotic theory of multidimensional detonation with an embedded sonic locus. (in preparation)

[14] Klein, R. & Stewart D. S. 1993 The relation between curvature, rate state-dependence and detonation velocity. *SIAM J. Appl. Maths* **53**, 1401-1435.
[15] Korobeinikov, V. P. 1991 *Problems of point-blast theory*. American Institute of Physics.
[16] Lee, J. H. S. 1977 Initiation of gaseous detonation. *Ann. Rev. Phys. Chem.* **28**, 75-104.
[17] Lee, J. H. S. 1984 Dynamic parameters of gaseous detonations. *Ann. Rev. Fluid Mech.* **16**, 311-336.
[18] Lee, J. H. S. & Higgins, A. J. 1999 Comments on the criteria for direct initiation of detonation. *Phil. Trans. R. Soc. Lond.* A **357**, 3503-3521.
[19] Litchfield, E. L., Hay, M. H. & Forshey, D. R. 1962 Direct electrical initiation of freely expanding gaseous detonation waves. *Proc. Comb. Inst.* **9**, 282-286.
[20] Matsui, H. & Lee, J. H. S. 1979 On the measure of the relative detonation hazards of gaseous fuel-oxygen and air mixtures. *Proc. Combust. Inst.* **17**, 1269-1280.
[21] Short, M. & Bdzil, J. B. 2003 Propagation laws for steady curved detonations with chain-branching kinetics. *J. Fluid Mech.* **479**, 39-64.
[22] Stewart, D. S. & Bdzil, J. B. 1988a The shock dynamics of stable multi-dimensional detonation. *Combust. Flame* **72**, 311-323.
[23] Stewart, D. S. & Bdzil, J. B. 1988b A Lecture on Detonation Shock Dynamics. *Lecture Notes in Physics* **299**, 17-30. Springer.
[24] Stewart, D. S. & Kasimov, A. R. 2004 General theory of detonation with an embedded sonic locus. *SIAM J. Appl. Maths* (submitted).
[25] Stewart, D. S. & Yao, J. 1998 The normal detonation shock velocity - curvature relationship for materials with nonideal equation of state and multiple turning points. *Combust. Flame* **113**, 224-235.
[26] Wood, W. W. & Kirkwood, J. G. 1954 Diameter effect in condensed explosives. The relation between velocity and radius of curvature in the detonation wave. *J. Chem. Phys.* **22**, 1920-1924.
[27] Yao, J. & Stewart, D. S. 1995 On the normal detonation shock velocity curvature relationship for materials with large activation energy. *Combust. Flame*, **100**, 519-528.
[28] Yao, J. & Stewart, D. S. 1996 On the dynamics of multi-dimensional detonation waves. *J. Fluid Mech.* **309**, 225-275.

List of Recent TAM Reports

No.	Authors	Title	Date
958	Christensen, K. T., and R. J. Adrian	Statistical evidence of hairpin vortex packets in wall turbulence—*Journal of Fluid Mechanics* **431**, 433–443 (2001)	Oct. 2000
959	Kuznetsov, I. R., and D. S. Stewart	Modeling the thermal expansion boundary layer during the combustion of energetic materials—*Combustion and Flame*, in press (2001)	Oct. 2000
960	Zhang, S., K. J. Hsia, and A. J. Pearlstein	Potential flow model of cavitation-induced interfacial fracture in a confined ductile layer—*Journal of the Mechanics and Physics of Solids*, **50**, 549–569 (2002)	Nov. 2000
961	Sharp, K. V., R. J. Adrian, J. G. Santiago, and J. I. Molho	Liquid flows in microchannels—Chapter 6 of *CRC Handbook of MEMS* (M. Gad-el-Hak, ed.) (2001)	Nov. 2000
962	Harris, J. G.	Rayleigh wave propagation in curved waveguides—*Wave Motion* **36**, 425–441 (2002)	Jan. 2001
963	Dong, F., A. T. Hsui, and D. N. Riahi	A stability analysis and some numerical computations for thermal convection with a variable buoyancy factor—*Journal of Theoretical and Applied Mechanics* **2**, 19–46 (2002)	Jan. 2001
964	Phillips, W. R. C.	Langmuir circulations beneath growing or decaying surface waves—*Journal of Fluid Mechanics* (submitted)	Jan. 2001
965	Bdzil, J. B., D. S. Stewart, and T. L. Jackson	Program burn algorithms based on detonation shock dynamics—*Journal of Computational Physics* (submitted)	Jan. 2001
966	Bagchi, P., and S. Balachandar	Linearly varying ambient flow past a sphere at finite Reynolds number: Part 2—Equation of motion—*Journal of Fluid Mechanics* **481**, 105–148 (2003) (with change in title)	Feb. 2001
967	Cermelli, P., and E. Fried	The evolution equation for a disclination in a nematic fluid—*Proceedings of the Royal Society A* **458**, 1–20 (2002)	Apr. 2001
968	Riahi, D. N.	Effects of rotation on convection in a porous layer during alloy solidification—Chapter 12 in *Transport Phenomena in Porous Media* (D. B. Ingham and I. Pop, eds.), 316–340 (2002)	Apr. 2001
969	Damljanovic, V., and R. L. Weaver	Elastic waves in cylindrical waveguides of arbitrary cross section—*Journal of Sound and Vibration* (submitted)	May 2001
970	Gioia, G., and A. M. Cuitiño	Two-phase densification of cohesive granular aggregates—*Physical Review Letters* **88**, 204302 (2002) (in extended form and with added co-authors S. Zheng and T. Uribe)	May 2001
971	Subramanian, S. J., and P. Sofronis	Calculation of a constitutive potential for isostatic powder compaction—*International Journal of Mechanical Sciences* (submitted)	June 2001
972	Sofronis, P., and I. M. Robertson	Atomistic scale experimental observations and micromechanical/continuum models for the effect of hydrogen on the mechanical behavior of metals—*Philosophical Magazine* (submitted)	June 2001
973	Pushkin, D. O., and H. Aref	Self-similarity theory of stationary coagulation—*Physics of Fluids* **14**, 694–703 (2002)	July 2001
974	Lian, L., and N. R. Sottos	Stress effects in ferroelectric thin films—*Journal of the Mechanics and Physics of Solids* (submitted)	Aug. 2001
975	Fried, E., and R. E. Todres	Prediction of disclinations in nematic elastomers—*Proceedings of the National Academy of Sciences* **98**, 14773–14777 (2001)	Aug. 2001
976	Fried, E., and V. A. Korchagin	Striping of nematic elastomers—*International Journal of Solids and Structures* **39**, 3451–3467 (2002)	Aug. 2001
977	Riahi, D. N.	On nonlinear convection in mushy layers: Part I. Oscillatory modes of convection—*Journal of Fluid Mechanics* **467**, 331–359 (2002)	Sept. 2001
978	Sofronis, P., I. M. Robertson, Y. Liang, D. F. Teter, and N. Aravas	Recent advances in the study of hydrogen embrittlement at the University of Illinois—Invited paper, Hydrogen–Corrosion Deformation Interactions (Sept. 16–21, 2001, Jackson Lake Lodge, Wyo.)	Sept. 2001

List of Recent TAM Reports (cont'd)

No.	*Authors*	*Title*	*Date*
979	Fried, E., M. E. Gurtin, and K. Hutter	A void-based description of compaction and segregation in flowing granular materials—*Continuum Mechanics and Thermodynamics*, in press (2003)	Sept. 2001
980	Adrian, R. J., S. Balachandar, and Z.-C. Liu	Spanwise growth of vortex structure in wall turbulence—*Korean Society of Mechanical Engineers International Journal* **15**, 1741–1749 (2001)	Sept. 2001
981	Adrian, R. J.	Information and the study of turbulence and complex flow—*Japanese Society of Mechanical Engineers Journal B*, in press (2002)	Oct. 2001
982	Adrian, R. J., and Z.-C. Liu	Observation of vortex packets in direct numerical simulation of fully turbulent channel flow—*Journal of Visualization*, in press (2002)	Oct. 2001
983	Fried, E., and R. E. Todres	Disclinated states in nematic elastomers—*Journal of the Mechanics and Physics of Solids* **50**, 2691–2716 (2002)	Oct. 2001
984	Stewart, D. S.	Towards the miniaturization of explosive technology—Proceedings of the 23rd International Conference on Shock Waves (2001)	Oct. 2001
985	Kasimov, A. R., and Stewart, D. S.	Spinning instability of gaseous detonations—*Journal of Fluid Mechanics* (submitted)	Oct. 2001
986	Brown, E. N., N. R. Sottos, and S. R. White	Fracture testing of a self-healing polymer composite—*Experimental Mechanics* (submitted)	Nov. 2001
987	Phillips, W. R. C.	Langmuir circulations—*Surface Waves* (J. C. R. Hunt and S. Sajjadi, eds.), in press (2002)	Nov. 2001
988	Gioia, G., and F. A. Bombardelli	Scaling and similarity in rough channel flows—*Physical Review Letters* **88**, 014501 (2002)	Nov. 2001
989	Riahi, D. N.	On stationary and oscillatory modes of flow instabilities in a rotating porous layer during alloy solidification—*Journal of Porous Media* **6**, 1–11 (2003)	Nov. 2001
990	Okhuysen, B. S., and D. N. Riahi	Effect of Coriolis force on instabilities of liquid and mushy regions during alloy solidification—*Physics of Fluids* (submitted)	Dec. 2001
991	Christensen, K. T., and R. J. Adrian	Measurement of instantaneous Eulerian acceleration fields by particle-image accelerometry: Method and accuracy—*Experimental Fluids* (submitted)	Dec. 2001
992	Liu, M., and K. J. Hsia	Interfacial cracks between piezoelectric and elastic materials under in-plane electric loading—*Journal of the Mechanics and Physics of Solids* **51**, 921–944 (2003)	Dec. 2001
993	Panat, R. P., S. Zhang, and K. J. Hsia	Bond coat surface rumpling in thermal barrier coatings—*Acta Materialia* **51**, 239–249 (2003)	Jan. 2002
994	Aref, H.	A transformation of the point vortex equations—*Physics of Fluids* **14**, 2395–2401 (2002)	Jan. 2002
995	Saif, M. T. A, S. Zhang, A. Haque, and K. J. Hsia	Effect of native Al_2O_3 on the elastic response of nanoscale aluminum films—*Acta Materialia* **50**, 2779–2786 (2002)	Jan. 2002
996	Fried, E., and M. E. Gurtin	A nonequilibrium theory of epitaxial growth that accounts for surface stress and surface diffusion—*Journal of the Mechanics and Physics of Solids* **51**, 487–517 (2003)	Jan. 2002
997	Aref, H.	The development of chaotic advection—*Physics of Fluids* **14**, 1315–1325 (2002); see also *Virtual Journal of Nanoscale Science and Technology*, 11 March 2002	Jan. 2002
998	Christensen, K. T., and R. J. Adrian	The velocity and acceleration signatures of small-scale vortices in turbulent channel flow—*Journal of Turbulence*, in press (2002)	Jan. 2002
999	Riahi, D. N.	Flow instabilities in a horizontal dendrite layer rotating about an inclined axis—*Journal of Porous Media*, in press (2003)	Feb. 2002
1000	Kessler, M. R., and S. R. White	Cure kinetics of ring-opening metathesis polymerization of dicyclopentadiene—*Journal of Polymer Science A* **40**, 2373–2383 (2002)	Feb. 2002
1001	Dolbow, J. E., E. Fried, and A. Q. Shen	Point defects in nematic gels: The case for hedgehogs—*Proceedings of the National Academy of Sciences* (submitted)	Feb. 2002

List of Recent TAM Reports (cont'd)

No.	*Authors*	*Title*	*Date*
1002	Riahi, D. N.	Nonlinear steady convection in rotating mushy layers—*Journal of Fluid Mechanics* **485**, 279–306 (2003)	Mar. 2002
1003	Carlson, D. E., E. Fried, and S. Sellers	The totality of soft-states in a neo-classical nematic elastomer—*Journal of Elasticity* **69**, 169–180 (2003) with revised title	Mar. 2002
1004	Fried, E., and R. E. Todres	Normal-stress differences and the detection of disclinations in nematic elastomers—*Journal of Polymer Science B: Polymer Physics* **40**, 2098–2106 (2002)	June 2002
1005	Fried, E., and B. C. Roy	Gravity-induced segregation of cohesionless granular mixtures—*Lecture Notes in Mechanics*, in press (2002)	July 2002
1006	Tomkins, C. D., and R. J. Adrian	Spanwise structure and scale growth in turbulent boundary layers—*Journal of Fluid Mechanics* (submitted)	Aug. 2002
1007	Riahi, D. N.	On nonlinear convection in mushy layers: Part 2. Mixed oscillatory and stationary modes of convection—*Journal of Fluid Mechanics* (submitted)	Sept. 2002
1008	Aref, H., P. K. Newton, M. A. Stremler, T. Tokieda, and D. L. Vainchtein	Vortex crystals—*Advances in Applied Mathematics* **39**, in press (2002)	Oct. 2002
1009	Bagchi, P., and S. Balachandar	Effect of turbulence on the drag and lift of a particle—*Physics of Fluids*, in press (2003)	Oct. 2002
1010	Zhang, S., R. Panat, and K. J. Hsia	Influence of surface morphology on the adhesive strength of aluminum/epoxy interfaces—*Journal of Adhesion Science and Technology* **17**, 1685–1711 (2003)	Oct. 2002
1011	Carlson, D. E., E. Fried, and D. A. Tortorelli	On internal constraints in continuum mechanics—*Journal of Elasticity* **70**, 101–109 (2003)	Oct. 2002
1012	Boyland, P. L., M. A. Stremler, and H. Aref	Topological fluid mechanics of point vortex motions—*Physica D* **175**, 69–95 (2002)	Oct. 2002
1013	Bhattacharjee, P., and D. N. Riahi	Computational studies of the effect of rotation on convection during protein crystallization—*Journal of Crystal Growth* (submitted)	Feb. 2003
1014	Brown, E. N., M. R. Kessler, N. R. Sottos, and S. R. White	*In situ* poly(urea-formaldehyde) microencapsulation of dicyclopentadiene—*Journal of Microencapsulation* (submitted)	Feb. 2003
1015	Brown, E. N., S. R. White, and N. R. Sottos	Microcapsule induced toughening in a self-healing polymer composite—*Journal of Materials Science* (submitted)	Feb. 2003
1016	Kuznetsov, I. R., and D. S. Stewart	Burning rate of energetic materials with thermal expansion—*Combustion and Flame* (submitted)	Mar. 2003
1017	Dolbow, J., E. Fried, and H. Ji	Chemically induced swelling of hydrogels—*Journal of the Mechanics and Physics of Solids*, in press (2003)	Mar. 2003
1018	Costello, G. A.	Mechanics of wire rope—Mordica Lecture, Interwire 2003, Wire Association International, Atlanta, Georgia, May 12, 2003	Mar. 2003
1019	Wang, J., N. R. Sottos, and R. L. Weaver	Thin film adhesion measurement by laser induced stress waves—*Journal of the Mechanics and Physics of Solids* (submitted)	Apr. 2003
1020	Bhattacharjee, P., and D. N. Riahi	Effect of rotation on surface tension driven flow during protein crystallization—*Microgravity Science and Technology* **14**, 36–44 (2003)	Apr. 2003
1021	Fried, E.	The configurational and standard force balances are not always statements of a single law—*Proceedings of the Royal Society* (submitted)	Apr. 2003
1022	Panat, R. P., and K. J. Hsia	Experimental investigation of the bond coat rumpling instability under isothermal and cyclic thermal histories in thermal barrier systems—*Proceedings of the Royal Society of London A*, in press (2003)	May 2003
1023	Fried, E., and M. E. Gurtin	A unified treatment of evolving interfaces accounting for small deformations and atomic transport: grain-boundaries, phase transitions, epitaxy—*Advances in Applied Mechanics*, in press (2003)	May 2003

List of Recent TAM Reports (cont'd)

No.	*Authors*	*Title*	*Date*
1024	Dong, F., D. N. Riahi, and A. T. Hsui	On similarity waves in compacting media—*Horizons in Physics*, in press (2003)	May 2003
1025	Liu, M., and K. J. Hsia	Locking of electric field induced non-180° domain switching and phase transition in ferroelectric materials upon cyclic electric fatigue—*Applied Physics Letters*, in press (2003)	May 2003
1026	Liu, M., K. J. Hsia, and M. Sardela Jr.	In situ X-ray diffraction study of electric field induced domain switching and phase transition in PZT-5H—*Journal of the American Ceramics Society* (submitted)	May 2003
1027	Riahi, D. N.	On flow of binary alloys during crystal growth—*Recent Research Development in Crystal Growth*, in press (2003)	May 2003
1028	Riahi, D. N.	On fluid dynamics during crystallization—*Recent Research Development in Fluid Dynamics*, in press (2003)	July 2003
1029	Fried, E., V. Korchagin, and R. E. Todres	Biaxial disclinated states in nematic elastomers—*Journal of Chemical Physics* **119**, 13170–13179 (2003)	July 2003
1030	Sharp, K. V., and R. J. Adrian	Transition from laminar to turbulent flow in liquid filled microtubes—*Physics of Fluids* (submitted)	July 2003
1031	Yoon, H. S., D. F. Hill, S. Balachandar, R. J. Adrian, and M. Y. Ha	Reynolds number scaling of flow in a Rushton turbine stirred tank: Part I—Mean flow, circular jet and tip vortex scaling—*Chemical Engineering Science* (submitted)	Aug. 2003
1032	Raju, R., S. Balachandar, D. F. Hill, and R. J. Adrian	Reynolds number scaling of flow in a Rushton turbine stirred tank: Part II—Eigen-decomposition of fluctuation—*Chemical Engineering Science* (submitted)	Aug. 2003
1033	Hill, K. M., G. Gioia, and V. V. Tota	Structure and kinematics in dense free-surface granular flow—*Physical Review Letters*, in press (2003)	Aug. 2003
1034	Fried, E., and S. Sellers	Free-energy density functions for nematic elastomers—*Journal of the Mechanics and Physics of Solids*, in press (2003)	Sept. 2003
1035	Kasimov, A. R., and D. S. Stewart	On the dynamics of self-sustained one-dimensional detonations: A numerical study in the shock-attached frame—*Physics of Fluids* (submitted)	Nov. 2003
1036	Fried, E., and B. C. Roy	Disclinations in a homogeneously deformed nematic elastomer—*Nature Materials* (submitted)	Nov. 2003
1037	Fried, E., and M. E. Gurtin	The unifying nature of the configurational force balance—*Mechanics of Material Forces* (P. Steinmann and G. A. Maugin, eds.), in press (2003)	Dec. 2003
1038	Panat, R., K. J. Hsia, and J. W. Oldham	Rumpling instability in thermal barrier systems under isothermal conditions in vacuum—*Philosophical Magazine* (submitted)	Dec. 2003
1039	Cermelli, P., E. Fried, and M. E. Gurtin	Sharp-interface nematic–isotropic phase transitions without flow—*Archive for Rational Mechanics and Analysis* (submitted)	Dec. 2003
1040	Yoo, S., and D. S. Stewart	A hybrid level-set method in two and three dimensions for modeling detonation and combustion problems in complex geometries—*Combustion Theory and Modeling* (submitted)	Feb. 2004
1041	Dienberg, C. E., S. E. Ott-Monsivais, J. L. Ranchero, A. A. Rzeszutko, and C. L. Winter	Proceedings of the Fifth Annual Research Conference in Mechanics (April 2003), TAM Department, UIUC (E. N. Brown, ed.)	Feb. 2004
1042	Kasimov, A. R., and D. Scott Stewart	Asymptotic theory of ignition and failure of self-sustained detonations—*Journal of Fluid Mechanics* (submitted)	Feb. 2004